



Universidade de Aveiro
Ano 2012/2013

Departamento de Química

**JOÃO ANTÓNIO
CORREIA FRAGOSO
FERNANDES**

**ESPECIAÇÃO DO FERRO DURANTE A
DIGESTÃO DE ALIMENTOS DE ORIGEM
VEGETAL**





Universidade de Aveiro
Ano 2012/2013

Departamento de Química

**JOÃO ANTÓNIO
CORREIA FRAGOSO
FERNANDES**

**IRON SPECIATION DURING THE
DIGESTION OF PLANT-BASED FOODS**





Universidade de Aveiro
Ano 2012/2013

Departamento de Química

**JOÃO ANTÓNIO
CORREIA FRAGOSO
FERNANDES**

**ESPECIAÇÃO DO FERRO DURANTE A
DIGESTÃO DE ALIMENTOS DE ORIGEM
VEGETAL**

Dissertação apresentada à Universidade de Aveiro para cumprimento dos requisitos necessários à obtenção do grau de Mestre em Química – ramo de Química Analítica e Qualidade, realizada sob a orientação científica da Doutora Sylvaine Bruggraber, Investigadora do Medical Research Council – Human Nutrition Research, do Doutor Brian James Goodfellow, Professor Auxiliar do Departamento de Química da Universidade de Aveiro e do Doutor Jorge Manuel Alexandre Saraiva, Investigador Auxiliar do Departamento de Química da Universidade de Aveiro



o júri

Doutor Artur Manuel Soares de Silva
Professor Catedrático do Departamento de Química da Universidade de Aveiro

Doutora Teresa Margarida Santos
Professora Auxiliar do Departamento de Química da Universidade de Aveiro

Doutor Nuno Jorge Rodrigues Faria
Investigador do Medical Research Council-Human Nutrition Research

Doutor Brian James Goodfellow
Professor Auxiliar do Departamento de Química da Universidade de Aveiro

Doutor Jorge Manuel Alexandre Saraiva
Investigador Auxiliar do Departamento de Química da Universidade de Aveiro

agradecimentos

Agradeço a todos os que me apoiaram durante este projecto, em especial aos meus pais por tornarem possível a minha vinda para Cambridge. No MRC-HNR, agradeço particularmente à Doutora Sylvaine Bruggraber, com quem aprendi muito, por me ter aceite e orientado neste projecto e pelo incrível apoio dado durante todo o seu desenvolvimento. Muito obrigado a todo o BMR pelo fantástico ambiente de trabalho que encontrei. Por último, agradeço ao Doutor Jonhathan Powell por me ter acolhido no seu grupo. Na Universidade de Aveiro, um especial obrigado ao Doutor Brian Goodfellow e ao Doutor Jorge Saraiva por todo o apoio dado durante este ano lectivo.

Palavras-chave Ferro, especiação, digestão, ferro não-heme, ferritina, nanopartículas de ferro

Resumo

Introdução: A Anemia de Deficiência de Ferro é um problema crítico à escala mundial. Apesar do ferro ser estudado extensivamente, muito ainda é desconhecido sobre a especiação do ferro não-heme durante a digestão e como isto afecta a sua biodisponibilidade. A ferritina é conhecida como uma proteína de armazenamento de ferro, mas como esta absorve o ferro ainda é um tópico controverso. A presença e a absorção de nanopartículas de ferro formadas naturalmente tem sido objecto recente de estudo.

Objectivo: O objectivo deste projecto é o estudo da especiação do ferro durante a digestão de alimentos de origem vegetal, com particular interesse para a absorção de ferro no duodeno, uma vez que é aqui que o ferro é absorvido e onde a especiação do ferro vai determinar a sua biodisponibilidade.

Métodos: Um sistema de digestão *in vitro* foi desenvolvido previamente no MRC-HNR, e neste projecto foi expandido e otimizado. Este sistema foi utilizado para a digestão de batatas e ervilhas. Para estudar a distribuição de fases do ferro foram utilizados diferentes filtros e centrifugações. Para a quantificação do ferro, as amostras foram digeridas em meio ácido com auxílio de microondas antes de análise por ICP-OES. Para uma caracterização mais aprofundada do conteúdo nanoparticulado, foram utilizadas as técnicas de SDS-PAGE e ICP-MS.

Resultados e discussão: Foi identificado que no duodeno a maioria do conteúdo de ferro proveniente de batatas e ervilhas apresenta-se em forma nanoparticulada. Posterior caracterização indicou que uma grande parte destas nanopartículas tem entre 2 e 14 nm. O conteúdo de ferro proveniente de FeCl_3 manifesta-se como precipitado ao nível do duodeno quando adicionado a batatas, e o conteúdo de ferro da ferritina manifesta-se como nanoparticulado.

Conclusão: Um sistema de digestão *in vitro* foi adaptado e otimizado para o estudo de alimentos de origem vegetal. Os estudos feitos neste sistema indicam que as batatas e as ervilhas são uma boa fonte de ferro biodisponível e podem ajudar na prevenção de deficiência de ferro.

Keywords

Iron, speciation, digestion, non-haem iron, ferritin, iron nanoparticles.

Abstract

Introduction: Iron Deficiency Anaemia is a critical problem in a worldwide scale. Even though iron has been extensively studied, not much is known of non-haem iron speciation during the digestion and how it affects bioavailability. Ferritin is known to be an iron storage protein, but the bioavailability of its iron content is still a controversial topic. The presence of naturally formed iron nanoparticles during digestion and how they might be absorbed has been hypothesized.

Aim: The aim of this project is to study iron speciation of plant-based foods during digestion, with particular interest to the duodenum since it is there that iron is absorbed and the iron speciation at this level will determine its bioavailability.

Methods: An *in vitro* digestion system has been previously developed at the MRC-HNR, and has been expanded and optimized for this project. Potato and peas have been digested. To study iron phases distribution, different filters and centrifugations were utilized on the digests. For the iron content quantification, the samples went through microwave-assisted acid digestion prior to ICP-OES analysis. To further characterise the nanoparticulated portions, SDS-PAGE and ICP-MS and were used.

Results and discussion: It has been found that at the duodenal level a majority of the iron content from digested potatoes and peas is present as nanoparticles. Further characterization indicates that a large part of these particles are between the sizes of 2 and 14 nm. When spiked on potatoes, the ferric iron from FeCl_3 precipitates, and the iron from ferritin becomes nanoparticulated.

Conclusion: An *in vitro* digestion system was adapted and optimized for the study of plant-based foods. The studies made in this system indicate that both potatoes and peas are a good source of bioavailable iron and thus can help in the prevention of iron deficiency.

Contents

List of Figures	11
1) Introduction.....	13
1.1) Biological iron.....	13
1.1.1) Biological functions of iron	13
1.1.2) Iron disorders	16
1.1.3) Dietary iron absorption: intake.....	18
1.1.4) Dietary iron absorption: efflux.....	22
1.2) Iron in food.....	23
1.2.1) Iron content in food	23
1.2.2) Iron chemistry	25
1.2.3) Digestion of iron.....	28
1.2.4) <i>In vitro</i> digestion	29
2) Iron speciation during the digestion of plant-based foods	31
2.1) Previous work.....	31
2.2) Aim of the project.....	31
3) Materials and Methods	33
3.1) Techniques	33
3.1.1) Microwave digestion	33
3.1.2) ICP-OES	34
3.2) Materials.....	35
3.2.1) Chemicals.....	35
3.2.2) Equipment	36
3.3) Methods.....	37
3.3.1) Sample preparation.....	37
3.3.2) Ferritin extraction.....	37
3.3.3) Protein content determination	38
3.3.4) Determination of iron content (ICP-OES)	39
3.3.5) Microwave-assisted acid digestion	40
3.3.6) <i>In vitro</i> digestion assays	40
3.3.7) <i>In vitro</i> digestion method development and optimization	42
3.3.8) Iron phase distribution and calculations.....	43
3.3.9) SDS-PAGE	46

3.3.10)	Determination of the iron content of the SDS-PAGE Gel Bands	46
4)	Results and Discussion	47
4.1)	Iron quantification of samples.....	47
4.1.1)	Potato samples	47
4.1.2)	Pea samples	47
4.2)	Ferritin characterization.....	47
4.3)	<i>In vitro</i> digestion assays	49
4.3.1)	Behaviour of ferric chloride in the <i>in vitro</i> digestion system.....	49
4.3.2)	Potato digestion	51
4.3.4)	Spiked potato digestion	55
4.3.5)	Pea digestion	58
4.3.6)	Spiked peas digestion.....	60
4.4)	Characterization of the nanoparticulated fraction.....	61
4.4.1)	Size distribution with ultrafiltration	61
4.4.2)	Gel electrophoresis	63
	Conclusions.....	68
	References	70

List of Figures

Figure 1: Distribution of iron in adults.	14
Figure 2: Molecular structure of haem and haemoglobin.	15
Figure 3: DMT1 pathway.	20
Figure 4: Possible ferritin uptake mechanisms.	21
Figure 5: Cellular mechanisms involved in intestinal iron absorption.	22
Figure 6: Solubility of iron and haem at various pH.	28
Figure 7: Schematic representation of an <i>in vitro</i> digestion system.	30
Figure 8: Ultrawave microwave digestion equipment, available at MRC-HNR.	33
Figure 9: ICP-OES Ultima (Horiba) available at MRC-HNR.	34
Figure 10: Samples used in this project.	37
Figure 11: Overview of the <i>in vitro</i> digestion system.	41
Figure 12: Phase distribution after <i>in vitro</i> digestion.	44
Figure 13: Process behind calculations of Fe content.	45
Figure 14: Bradford assay of extracted ferritin.	48
Figure 15: FeCl ₃ control Fe phase distribution after <i>in vitro</i> digestion.	50
Figure 16: Instant potato powder <i>in vitro</i> digestion Fe phase distribution.	52
Figure 17: Gastric (left) and intestinal (right) aliquots after <i>in vitro</i> digestion.	53
Figure 18: Ferritin <i>in vitro</i> digestion Fe phase distribution.	54
Figure 19: Phase distribution of potato powder spiked with ferritin.	55
Figure 20: Phase distribution of potato powder spiked with FeCl ₃	57
Figure 21: Comparison of different <i>in vitro</i> digestion experiments with instant potato powder, at the intestinal time point.	58
Figure 22: Phase distribution of peas.	59
Figure 23: Comparison of the phase distribution of intestinal <i>in vitro</i> digested potatoes and peas.	60
Figure 24: Phase distribution of peas spiked with ferritin.	60
Figure 25: Comparison of the phase distribution of intestinal <i>in vitro</i> digested peas and peas spiked with ferritin.	61
Figure 26: Different sized filters used in the supernatant of the intestinal phase.	62
Figure 27: BCA protein content analysis of the supernatant of an intestinal aliquote of a potato <i>in vitro</i> digestion.	63
Figure 28: SDS-PAGE stained for protein.	64
Figure 29: Fe content of SDS-PAGE gels measured by ICP-MS.	66

List of Tables

Table 1: Iron location in the human body.....	13
Table 2: Iron content in selected plant-based foods (extract).	23
Table 3: Iron content in selected animal foods (extract).	24
Table 4: Iron intakes required.....	25
Table 5: Chemicals used.....	35
Table 6: Equipment used.	36
Table 7: FeCl ₃ Fe distribution after <i>in vitro</i> digestion	50
Table 8: Fe distribution after <i>in vitro</i> digestion of instant potato powder	52
Table 9: Fe distribution after <i>in vitro</i> digestion of ferritin	55
Table 10: Fe distribution after <i>in vitro</i> digestion of instant potato powder spiked with ferritin	56
Table 11: Fe distribution after <i>in vitro</i> digestion of instant potato powder spiked with FeCl ₃	57
Table 12: Fe distribution after <i>in vitro</i> digestion of peas.....	59
Table 13: Fe distribution after <i>in vitro</i> digestion of peas spiked with ferritin	61
Table 14: Fe size distribution of the supernatant of the intestinal phase of an <i>in vitro</i> digested potatoes experiment using different sized filters.....	63

1) Introduction

1.1) Biological iron

1.1.1) Biological functions of iron

Iron has an important biological role due to its considerable reactivity, manifested in many processes as a reversible one electron oxidation-reduction reaction that has iron changing from ferrous (Fe^{2+}) to ferric (Fe^{3+}). This reactivity is used by most enzyme systems involving electron transport, oxygen carriage and iron transport across membranes. The high reactivity is also responsible for the toxicity seen in cases of iron overload¹. The complexity of this system, and the major problems caused by both deficiency and overload are managed by a specialized system in which storage, transport and concentration regulation are highly controlled.

Our bodies have roughly 3.5 g of iron, about 50 mg per kilogram². As can be seen in [Table 1](#), over 60% is in the form of haemoglobin of red blood cells, 25% is stored mainly in the liver. Some of the iron is in enzymes (5%) and in the myoglobin in muscles (8%). The remaining iron can be found in transit in the circulation bound to the plasma transport protein, transferrin¹.

[Table 1: Iron location in the human body.](#)

Iron location	Amount
Haemoglobin	60%
Stored in the liver	25%
Myoglobin	8%
Enzymes	5%
Transferrin	2%

The concentration of iron in the human body is maintained mostly by the regulation of the absorption of dietary iron in the small intestine³. Compared to other animals humans conserve body iron more efficiently⁴. Excess body iron is slowly excreted in

the absence of haemorrhage or haemosiderinuria, for example an adult man will only lose 1 mg of iron per day (equivalent of 0.025% of total body iron), and a woman twice that amount due to menstruation. The other losses of iron from the body are epithelium from skin and intestinal secretions⁴. In order for a balance to be made the absorption of iron must at least equal these losses, or surpass them in growing ages (see [Figure 1](#)). The excretion of iron from the body has a more passive role than absorption, since it never varies much if haemorrhage and haemosiderinuria are not

present⁵. The maximal daily loss of iron in these conditions is still only about 4 mg per day⁶.

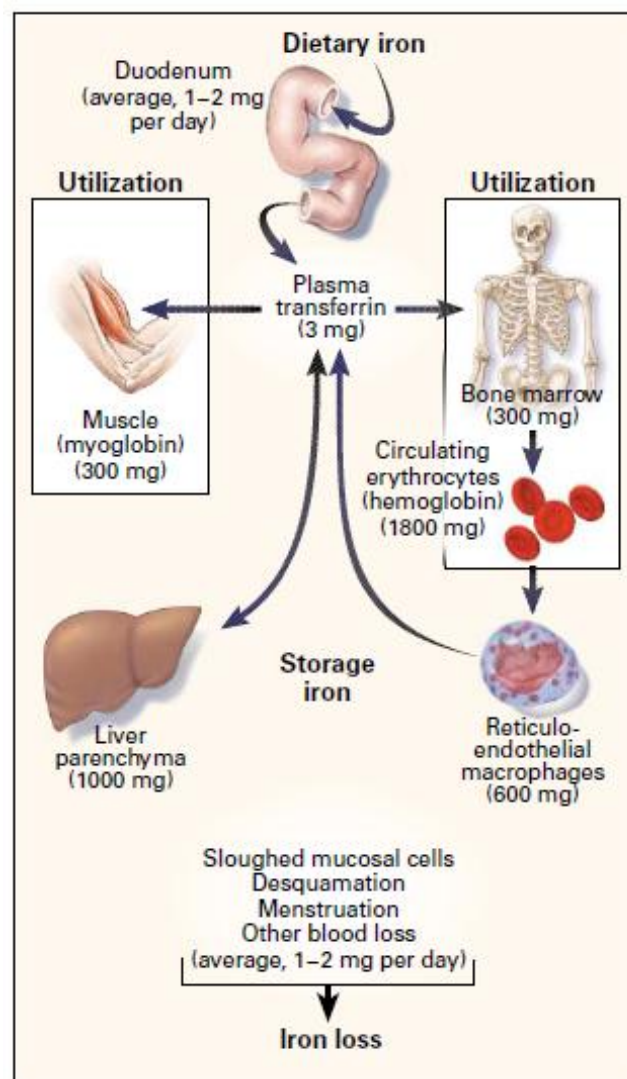


Figure 1: Distribution of iron in adults⁷.

Given the key role of iron in the structure and function of haemoglobin, its metabolic functions are one of the most studied among all the micronutrients. The main function of iron is related to the role of haemoglobin, transport of oxygen from the lungs to all tissues. Haemoglobin is composed from four globular protein subunits, each one of them with a haem group (Figure 2) connected to the polypeptide chain. Usually, there are 2 alpha chains that are each 141 amino acids long and 2 beta chains that are each 146 amino acids long. This arrangement will put the haem groups closely packed together (Figure 2)⁸.

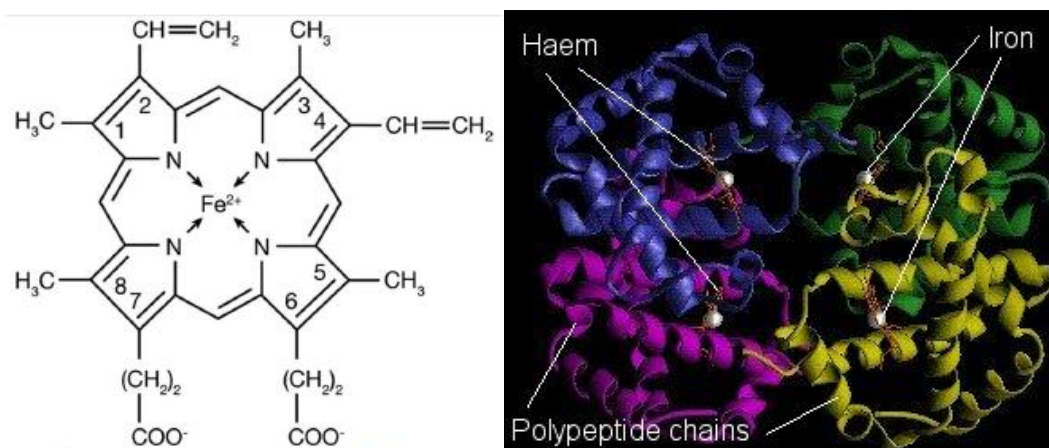


Figure 2: Molecular structure of haem² and haemoglobin⁹.

Each haem groups contains an iron ion held in a porphyrin ring. A porphyrin ring is composed of four pyrrole groups linked together with an iron ion bound in the centre. The iron ion is the oxygen binding site, and is coordinated with four nitrogens in the centre of the porphyrin ring. The iron is also bound covalently to the globular protein by an imidazole ring. The iron ion can be either in ferrous or ferric state, but only on ferrous state will it bind oxygen. The protein portion of haemoglobin and myoglobin prevents the oxidation of the ferrous iron and makes it possible for oxygen to bind reversibly to the haem group. Carbon dioxide is also transported by haemoglobin but it binds to the protein chains and not to the iron ions¹⁰. Carbon monoxide can bind to one of the oxygen binding sites in haemoglobin (haemoglobin has higher affinity to carbon monoxide than to oxygen)¹¹. There is also evidence that arsenic binds to the alpha-chain of haemoglobin¹².

Closely related to haemoglobin is myoglobin, a protein expressed in cardiac myocytes and oxidative skeletal muscle fibres. This protein has a single polypeptide chain folded around a haem group. As in haemoglobin, the iron ion interacts on four sides with nitrogen atoms, on a fifth side with the imidazole side chain of an amino acid and the sixth side serves as the binding site for oxygen¹³. Myoglobin's role is as an oxygen storage protein in muscle. This knowledge is supported by the fact that marine animals that undergo long periods of apnea have muscle myoglobin content of 10 to 30 fold compared to other animals¹³.

Haem groups can also be found in different proteins, such as for example cytochrome, giving it the capability to oxidize and reduce. Since cytochromes and other complexes are held within membranes in an organized way the redox reaction are held in a sequential and organized way. Iron is then an integral part of the oxidative phosphorylation which is the main energy generating process used by organisms which need oxygen⁸.

Another important biological role of iron is in the iron-sulphur clusters. These clusters were likely some of the first co-factors used by living organisms, ferrous iron and sulphide were highly available in the reducing atmosphere where life first evolved. Given the toxicity of both iron and free sulphide, it is easy to see why they were an evolutionary advantage¹⁴. Iron/sulphur clusters are versatile co-factors of proteins that mediate electron transfer, enzymatic catalysis and regulate gene expression. Research has found them to be required for complex I (NADH dehydrogenase) assembly¹⁵.

1.1.2) Iron disorders

Anaemia

Iron deficiency is a problem that affects a significant part of the population of the world, affecting more than half a billion people worldwide⁷. We define iron deficiency as the condition where there are no iron stores to be mobilized and where there are signs of a compromised supply of iron to the tissues. When this deficiency becomes more severe and haemoglobin concentrations become low we can say iron deficiency anaemia is present. Iron deficiency is characterized by changes in the amount of iron present in different compartments of the body. First, iron stores are depleted but there is still enough iron for red cell production. Only when the iron stores are completely exhausted do we reach iron deficient erythropoiesis, in which iron in circulation begins to decrease and red cell production is affected. The next step of deficiency is anaemia, in which the amount of iron in circulation is very low, red cell production is drastically reduced¹. Even though anaemia is the most common way to detect iron deficiency, less pronounced cases of iron deficiency without anaemia also merit attention, as tissues are still functionally impaired¹⁶.

Two factors that explain anaemia are the abnormal loss of iron, mainly by blood loss, and low uptake and absorption of iron. It is now apparent that in most developing countries the main factor contributing to iron deficiency is the poor bioavailability of iron in largely unrefined cereal-based diets¹. These factors explain the gender and geographical distribution of this disorder. A study of anaemia in women living in the United Kingdom from different ethnic origins found that women of Southeast Asian and Chinese origin had a higher rate of anaemia than other ethnic groups, and found that anaemia was more prevalent in woman who followed a vegetarian diet¹⁷.

Iron deficiency has been coupled with weakness and tiredness for a long time, and presently many adverse effects on human health have been observed and studied:

- Cognitive development: Iron has been shown to have a key role in brain function, and iron deficiency has been seen to delay psychomotor development and impair cognitive performance of infants in many different countries^{18, 19, 20, 21, 22}.
- Resistance to infection: Since iron has an adverse effect on the immune system²³, morbidity from infectious disease is increased in iron-deficient populations²⁴.
- Pregnancy: Iron deficiency is known to increase the incidence of prematurity, prenatal and peri-natal infant loss and maternal mortality²⁵.
- Productivity: The relationship between work capacity and iron deficiency has been studied in different countries^{26, 27}, and a linear relationship has been found.
- Growth: A link between iron deficiency and children growth has been found in different studies^{28, 29}.
- Production of neurotransmitters: Iron deficiency alters thyroid function, impairing the production of different neurotransmitters³⁰.

Overload

The most common iron overload disorder is genetic haemochromatosis. This recessive genetic disorder is more common in people of Northern European descent,

and is characterized by excessive hepatic iron accumulation from disruption of the regulation of intestinal iron absorption³¹. The body iron stores accumulate slowly, with clinical symptoms presenting themselves at the age of 40 – 60 years. Skin pigmentation, diabetes, liver disease and gonadal failure are typical, together with more non-specific complaints such as weakness, lethargy, and joint and abdominal pain. The iron overload first affects hepatocytes but later builds up in the pancreas, and by the time of diagnosis the body can have a 15 or 20 fold increase from normal levels³².

1.1.3) Dietary iron absorption: intake

In general terms, dietary iron is divided in two major groups: “haem iron”, the iron found in meat and meat derived products; and “non-haem iron”, which is mostly present in vegetables, cereals, beans, fruits and other plant based food, even though it is still present in small quantities in animal products. Non-haem iron can be in a number of forms, like iron oxides and salts to more complex organic chelates. In most diets non-haem iron is the form of iron most ingested, comprising around 90% of total daily iron intake. Even though haem iron is ingested in lower amounts it has a higher bioavailability (about 20–30%)³³ when compared to non-haem iron (1-10%)³⁴. Contrary to haem iron, non-haem iron absorption is highly influenced by other dietary components that can inhibit or enhance its bioavailability. Some inhibitors are phytates and polyphenolic compounds that can be found in all plant foods, and the most studied enhancer is ascorbic acid. An equimolar concentration of ascorbic acid has been found to counteract the inhibitory effect of phytates and polyphenols³⁵.

The absorption of iron is regulated at the duodenum level, and there are many factors that can affect its bioavailability, such as the iron content of foods, the type of iron present, and other dietary components. The absorption is also regulated with the metabolic demands that are related to the amount of iron stored in the body.

Ferrous and Ferric Iron

Most of the dietary non-haem iron is believed ingested in ferrous form. Ferric iron is thought to be non-available for absorption, since it precipitates at pH greater than 3. Therefore, it has to be converted to ferrous iron before it can be absorbed.

Some dietary components are able to perform the reduction of Fe^{3+} to Fe^{2+} , such as ascorbic acid³⁶ and amino acids such as cysteine³⁷ and histidine³⁸.

It is suggested that the action of these reducing agents takes place in gastric digestion, but it is still possible for ferric iron to be reduced when reaching the duodenal enterocytes. There have been studies that demonstrated the iron reducing capability of enterocytes in cultured intestinal cells³⁹. The enzyme responsible for this reduction has been identified as duodenal cytochrome b (Dcytb)⁴⁰. Like cytochrome b, Dcytb is a haem containing protein that has binding sites for ascorbic acid and semi-dehydroascorbate. This protein is expressed in the border membrane of duodenal enterocytes.

After being reduced from ferric to ferrous iron by either dietary reducing agents or Dcytb, the ferrous iron is able to act as a substrate for DMT1 (divalent metal transporter)⁴¹ (Figure 3), and join the labile iron pool inside the enterocyte. DMT1 is a highly hydrophobic protein whose expression has been shown to be regulated in response to iron status, rats that are made iron deficient have increased levels of DMT1 mRNA⁴¹. Other work has shown that antibodies to DMT1 can significantly inhibit iron absorption⁴².

The biological functions of DMT1 have been studied through phenotypic analysis of animal with spontaneous mutation in DMT1. These mutation have resulted in severe impairment of iron transport function⁴³. DMT1 has also been shown to promote the transport of other metals such as manganese, cobalt, cadmium, copper, lead and zinc⁴¹.

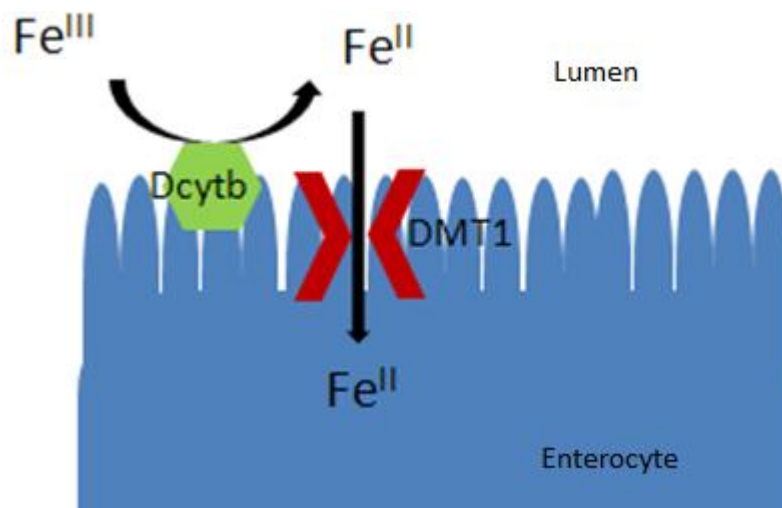


Figure 3: DMT1 pathway

There is an uncomfortable paradox with respect to Fe^{3+} absorption. Fe^{3+} is remarkably insoluble at duodenal pH, immediately precipitating out of solution as Fe^{3+} poly oxo-hydroxide. A new mechanism that attempts to explain the absorption of ferric iron as nanoparticles has been suggested by the Bio Mineral Research group in the MRC-HNR⁴⁴. It has been proposed that a range of endogenous, low molecular weight ligands could slow the rate of hydrolysis to allow Fe^{3+} binding to gastrointestinal mucins forming an impure Fe^{3+} poly-oxo-hydroxide. It has been shown that at duodenal conditions Fe^{3+} is not quite kept in solution but, rather, starts hydrolysis and the further growth and agglomeration of the Fe^{3+} poly oxo-hydroxide nanoparticles are prevented by mucin binding. Amorphous aggregates of Fe nanoparticles with ~10-20 nm have been visualized. Impurity and thus instability of the particles allows lysosomal processing and cellular utilization whilst its initial uptake is through epithelial cell membrane adhesion and endocytosis. This pathway would complement conventional DMT-1 transport of soluble Fe^{2+} and would not allow luminal redox activity, using the normal and safe compartment (lysosome) for Fe^{3+} cycling.

Ferritin

The most important iron storage protein in both animals and plants is ferritin. Every cell in animals and plants contains ferritin in small amounts⁴⁵. Ferritin is a protein-iron complex with a protein cage and a mineral core of thousands of ferric ions linked by oxygen atoms. There are studies that indicate that ferritin of both animal⁴⁶ and plant^{45, 47} sources have a good bioavailability. However, the

mechanism responsible for iron uptake is not currently known. Several mechanisms have been proposed. One possibility is that the outer protein structure of ferritin is broken down by protease activity releasing the iron inside, which could then be reduced to ferrous iron and be absorbed (Figure 4, A), but this is still a controversial subject, since *in vitro* studies have indicated that ferritin resists to high temperature, low pH and various denaturing agents⁴⁸. Another hypothesis is that ferritin is absorbed whole and broken down intracellularly to release its iron content (Figure 4, C), or that its protein shell might be broken down and only the iron core enters the enterocyte by some unknown mechanism (Figure 4, B).

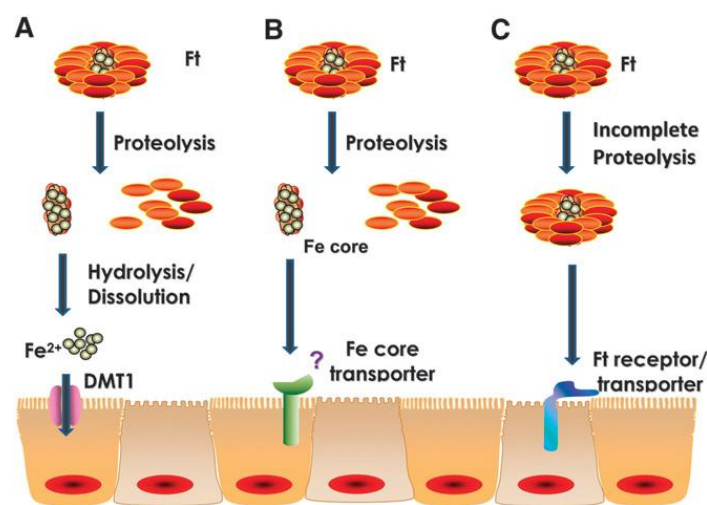


Figure 4: Possible ferritin uptake mechanisms⁴⁹

Ferritin has a unique structure among other proteins: The secondary, tertiary and quaternary structure is conserved (twenty four helix bundles assembled in a spherical protein cage with a large cavity), but except in higher plants and animals the amino acid sequence is highly variable⁴⁵. Still, overall, all ferritins have a spherical protein cage around a cavity where there is a nano mineral of hydrated ferric oxide.

Haem Iron

Haem is soluble at alkaline pH and precipitates under acid conditions. It has been observed that haem is taken up intact by the enterocytes but later appears in the plasma in a non-haem form, leading to the hypothesis that when it enters in contact with pancreatic enzymes it is released from haemoglobin and myoglobin⁵⁰. Globin degradation products are important because they help maintain haem in a de-

polymerized state making it available for absorption. Haem enters the enterocyte as an intact metalloporphyrin³, then being disassembled by haem oxygenase 1. Ultrastructural studies of haemoglobin indicate that the uptake of haem iron happen at least partially by endocytic processes⁵¹.

1.1.4) Dietary iron absorption: efflux

As we have seen, it is thought that all iron absorbed by the enterocytes is eventually in Fe^{2+} form, either by entering via DMT1 or after entering as whole haem and being disassembled inside the enterocytes by haem oxygenase 1. All this Fe^{2+} forms the common labile iron pool inside the enterocytes³⁴ (see Figure 5). From this labile pool there are two possible destinations, depending on the body iron stores: If these are high, the Fe^{2+} might be oxidized to Fe^{3+} and stored as ferritin inside the cell. If this is not the case it might be exported across the enterocyte's basolateral membrane⁵².

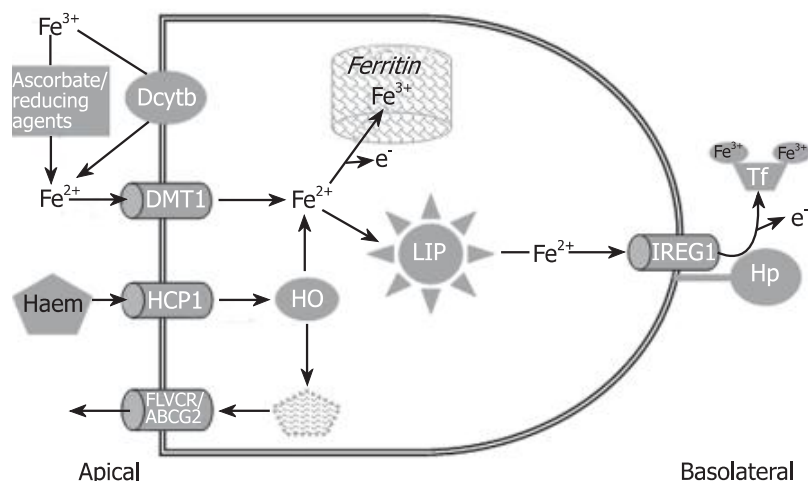


Figure 5: Cellular mechanisms involved in intestinal iron absorption³⁴.

The protein responsible for the transport of iron from the iron labile pool through the basolateral membrane into circulation has been identified as IREG1 (iron-regulated transporter 1), also known as ferroportin⁵³. IREG1 has no structural homology to DMT1. Like DMT1, IREG1 likely conducts Fe^{2+} ions. In order for iron to circulate bound to plasma proteins it needs to be oxidized to Fe^{3+} , and it appears that hephaestin is responsible for this function⁵⁴. Fe^{3+} is then quickly bound to transferrin, an abundant high-affinity iron binding protein which is responsible for transporting all the iron in the serum⁵⁵.

1.2) Iron in food

1.2.1) Iron content in food

Iron content varies greatly in different food, both in total iron content and also in which form iron is present. The bioavailability of the iron will also depend on further factors, such as other dietary components that enhance or inhibit the absorption, such as phytates and ascorbic acid. Food processing and preparation, together with changes in the iron during digestion will also play a key role in iron bioavailability.

It has been postulated that the iron content in some foods could have changed, due to changes in agricultural practices that could deplete the soils of important minerals⁵⁶. Here in the MRC–HNR an analysis of the iron content of plant-based foods in the United Kingdom was made⁵⁷, and its results were compared with previous studies (spanning 70 years). The study found remarkable consistency between the iron-content of food across the different studies along the years. Some of its results are in [Table 2](#). The small differences found are therefore unlikely to relate to a significant difference in total daily iron intake. Even if some foods have slightly lower iron content nowadays, this is likely compensated by the now prevalent iron fortification that occurs in certain foods, such as breakfast cereals and bread⁵⁷.

[Table 2: Iron content in selected plant-based foods \(extract\)⁵⁷.](#)

Food description	Fe content (mg/100g)
Bran flakes	59.35
Bread, brown	2.31
Bread, white	1.82
Bread, wholemeal	3.40
Breads, buttery (for example, croissants or brioche)	0.77
Cornflakes	14.81
Pasta, fusilli twists, white, cooked	0.48
Pasta, spaghetti, whole-wheat, boiled	1.49
Rice, jasmine, boiled	0.17
Rice, white, long-grain, boiled	0.39
Apples, eating, raw	0.13
Banana, raw	0.24
Kiwi fruit, fresh, raw, without skin	0.46

Orange, fresh, raw	0.24
Strawberries, raw	0.34
Black-eye beans, boiled	2.24
Red kidney beans, canned or dried and boiled	2.19
Chickpeas, canned or dried and boiled	1.42
Lentils, green and brown, boiled	4.18
Soya beans, dried and boiled	2.80
Tofu	3.05
Broccoli, green, fresh, boiled	0.70
Mushrooms, common and closed cup, fresh, raw	0.47
Onion, normal, fresh, raw	0.43
Peas, fresh, boiled	1.51
Peppers, green, fresh, raw	1.04
Potato, fresh, peeled, boiled	0.85
Salad, mixed leaves, fresh, raw	1.01
Spinach, fresh, boiled	3.85

As said before another important source of iron available to non-vegetarians is haem iron, which can be found in animal products. In [Table 3](#) we can see some of the results of a study of iron content in animal products⁵⁸:

[Table 3: Iron content in selected animal foods \(extract\)⁵⁸.](#)

Food description	Fe content (mg/100g)
Beef loin, raw	2.1
Chicken breast, raw	0.4
Chicken drumsticks, raw	1.2
Pork loin, raw	2.4
Freshwater catfish, raw	1.9
Red snapper, raw	1.2
Giant tiger prawn, raw	0.4

The Food and Agriculture Organization of the United Nations has compiled a list of the recommended requirements of iron intake per day. Looking at [Table 4](#) we see that the iron requirements change with age and sex. The daily recommended requirement is calculated taking into account the basal iron losses, the required iron intake for growth and the menstrual losses.

Table 4: Iron intakes required⁵⁹

Group	Age	Body weight	Required Iron intakes for Growth	Basal Iron losses	Menstrual losses	Total Absolute Requirements
		Mean		Median	Median	Median
	(Years)	(kg)	(mg/day)	(mg/day)	(mg/day)	(mg/day)
Children	0.5 to 1	9	0.55	0.17		0.72
	1 to 3	13.3	0.27	0.19		0.46
	4 to 6	19.2	0.23	0.27		0.5
	6 to 10	28.1	0.32	0.39		0.71
Males	11 to 14	45	0.55	0.62		1.17
	15-17	64.4	0.6	0.9		1.5
	18+	75		1.05		1.05
Females	11 to 14	46.1	0.55	0.65		1.2
	11 to 14	46.1	0.55	0.65	0.48	1.68
	15-17	56.4	0.35	0.79	0.48	1.62
	18+	62		0.87	0.48	1.46
Post-menopausal		62		0.87		0.87
Lactating		62		1.15		1.15

1.2.2) Iron chemistry

We can summarize most of the biological functions of iron according to three general reaction types: oxidation-reduction, hydrolysis and polynuclear complex formation.

Oxidation-reduction chemistry of iron

When in an aqueous solution iron is mostly divided between two oxidation states, ferrous iron (Fe^{2+}) and ferric iron (Fe^{3+}). Ferrous iron precipitates and is rendered unavailable for absorption at near neutral pH, but ferric iron precipitates more easily, at pH greater than three³.

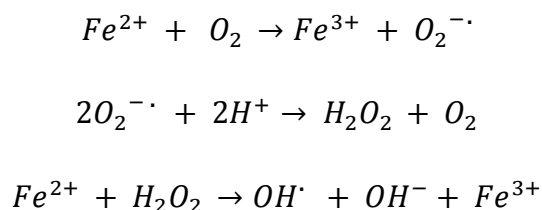
Transfer between these two states is accomplished in a variety of ways. Reducing agents such as ascorbic acid will usually convert aqueous ferric iron to ferrous iron, and molecular oxygen promotes the reverse reaction. For many biological manifestations of iron redox chemistry is easily accomplished and

reversible. For these reactions to be reversible the reduction potential of complexed iron needs to be within the range of biological oxidants: +820 mV (reduction potential of molecular oxygen at pH 7) to reductants -320 mV (reduction potential of pyridine nucleotides)⁶⁰. Some redox reaction may be irreversible if the reduction potential is outside of this range.

Considering normal physiological concentrations of oxygen, in most biological complexes the stable state of iron is Fe^{3+} . Since many biological processes make use of ferrous iron, the reduction of ferric to ferrous is a reaction of critical importance. Some of the processes that require ferrous iron are:

- 1) Haem synthesis – studies of ferrochelatase have shown that this enzyme catalyses one of the steps of haem synthesis, in which ferrous iron takes part^{61, 62};
- 2) Ferrous iron takes an integral part in the deposition of iron in the storage protein ferritin⁶³;
- 3) Transmembrane transport of iron – Even though iron absorption in the intestine is not a fully comprehended process, studies have shown that ferric iron needs to be reduced to ferrous by ferrireductases such as ascorbic acid before absorption^{41, 64, 65}.

The redox capabilities of iron also explain its toxicity. The reduction of molecular oxygen by Fe^{2+} form superoxides, which in turn leads to the formation of hydroxyl radicals. The formation of this hydroxyl radicals are explained by the Haber-Weiss-Fenton reaction sequence:

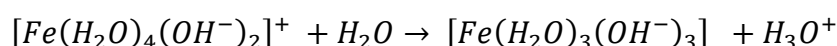
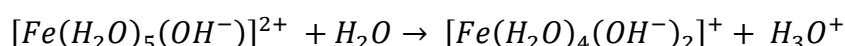
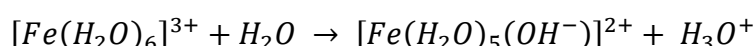


Hydroxyl radicals are extremely reactive, causing lipid peroxidation, DNA strand breaks and degradation of other biomolecules^{66, 67}. To minimize the formation of these radicals in the human body, iron binding proteins provide some defence mechanisms. Both transferrin and intracellular ferritin retain iron in safe Fe^{3+} form, which will not catalyse the production of free radicals unless mobilized. Ferritin's

protective ability is due to its ability to transform the more dangerous Fe^{2+} into the less toxic Fe^{3+} , conserving it inside its structure⁴⁸.

Hydrolysis chemistry of iron

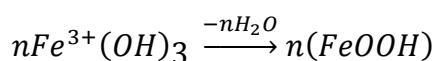
In acid solutions of pH <1.0, ferric and ferrous iron exist as the complexes $[\text{Fe}(\text{H}_2\text{O})_6]^{2+}$ and $[\text{Fe}(\text{H}_2\text{O})_6]^{3+}$. If autoxidation is prevented by low oxygen availability these aquated forms of iron persist through the pH of biological systems. However if this is not the case and the pH is raised above 2.0 the complex $[\text{Fe}(\text{H}_2\text{O})_6]^{3+}$ goes through a series of hydrolytic deprotonations⁶⁰:



The uncharged $[\text{Fe}(\text{H}_2\text{O})_3(\text{OH})_3]$ species is very insoluble (the maximum concentration of aquated Fe^{3+} at neutral pH is only about $10^{-17} \text{ mol L}^{-1}$), while the total concentration of Fe^{3+} in solution, mainly $[\text{Fe}(\text{H}_2\text{O})_4(\text{OH}^-)_2]^+$, is close to $10^{-9} \text{ mol L}^{-1}$. The insolubility of ferric hydroxide enhances autoxidation of Fe^{2+} .

Polynuclear complex formation

The last general reaction type used to explain the biological functions of iron is polynuclear complex formation. Hydroxide complexes of iron are easily polymerized by dehydration forming polynuclear complexes with iron atoms linked by oxo- or hydroxo-bridges⁶⁰:



These iron polymers in biological systems have from two iron atoms (as in proteins like ribonucleotide reductase) to complex three dimensional arrays of more than 4000 iron atoms (as happens in ferritin).

1.2.3) Digestion of iron

During digestion in the human body, the various forms of iron enter in contact with various enzymes, suffer mechanical breakdown and also enter in contact with solutions with variable acidity. Even knowing exactly what is the speciation of iron prior to ingestion, to study bioavailability of iron we need to know exactly what changes occur to iron during digestion.

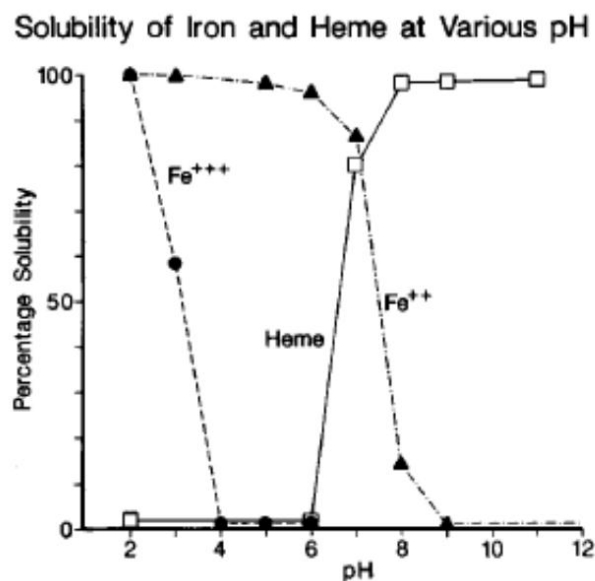


Figure 6: Solubility of iron and haem at various pH⁶⁸.

Given that almost all absorption of iron takes place at the duodenum, it is essential to know what form the iron has when it gets there. Critical for this evaluation is how the different forms of iron react to different levels of acidity (Figure 6). Haem iron is soluble at the pH present in the duodenum (pH about 6.5)⁶⁸, and mechanisms for its absorption have been proposed. Haem is freed from myoglobin and haemoglobin largely by pancreatic enzymes; Globin degradation products maintain haem in a de-polymerized state, making it available for absorption³.

Both ferrous and ferric salts are soluble in a gastric environment (with pH around 2). As the pH is raised in the duodenum, ferric iron forms large molecular weight polymers which precipitate. This precipitation will likely decrease bioavailability, but can be prevented by chelating agents such as ascorbic acid and citric acid⁶⁹.

What happens to ferritin during digestion is still a matter of debate. Some studies indicate absorption rates comparable to ferrous sulphate, the golden standard of iron absorption^{46, 70} while others indicate poor absorption^{71, 72}. It is also a matter of debate whether ferritin is broken down prior to absorption⁷³ or if it enters whole in the enterocytes.

1.2.4) *In vitro* digestion

The study of speciation of iron during digestion *in vivo* is a complicated task, particularly in human subjects. Even animal subjects present practical problems. One study, aiming to study iron in gastric and intestinal digestion of rats⁷⁴ involved removing the stomach and intestines in order to study its contents at different stages of digestion. *In vitro* methods offer an interesting alternative to human and animal studies. They can be simple, fast and inexpensive, allowing for multiple simultaneous experiments with different conditions.

Several *in vitro* digestion systems have been developed, with different aims. Some wanted to simulate the quantitative release of nutrients^{75, 76}, and others wanted to predict the glycaemic indexes⁷⁷. Most developed methods follow the same two main phases, with more or less automation: a gastric phase, where the food is mixed with a biological buffer at a low pH and where appropriate enzymes such as pepsin are added. The following step is intestinal, where pH is raised and pancreatin and bile salts are added⁷⁸.

In order to better simulate the full digestion process, attempts have been made to also include a simulation of digestion in the mouth with a buccal step. For this to happen, both the mechanical aspect and the chemical changes need to be taken into account. Various approaches have been tried, including having the food be chewed by subjects before entering the *in-vitro* system⁷⁹, incubating the samples with human saliva⁸⁰ and using mechanical mincers and amylase⁷⁷. Hoebler et al. has developed a comprehensive and mostly automated *in vitro* digested system which covers all three main phases of *in vivo* digestion (Figure 7). The buccal phase is done outside the system but gastric and intestinal phases are automated and account for variables such as pH, volume, temperature and time.

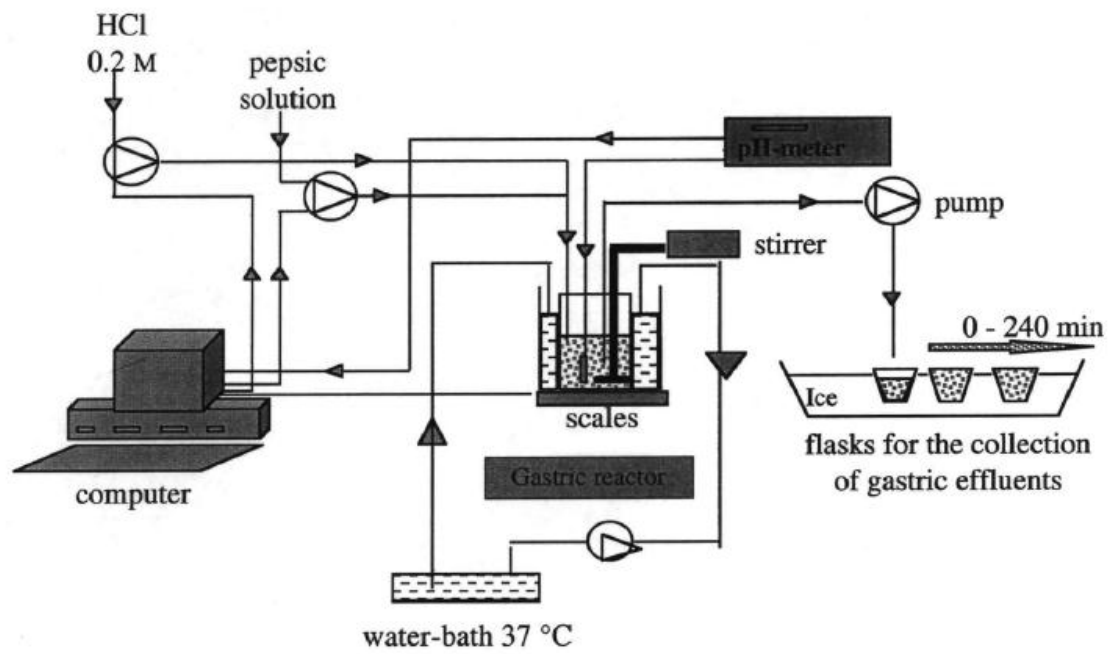


Figure 7: Schematic representation of an *in-vitro* digestion system⁸¹.

2) Iron speciation during the digestion of plant-based foods

2.1) Previous work

This project is a continuation of work previously carried in the Biomineral Research group of the Medical Research Council - Human Nutrition Research, which aims to study what is happening to iron during the digestion of plant-based food.

Karin Embacher was a MSc student whose thesis had the topic “The organic acid profile of the potato vacuole analysed by capillary electrophoresis and how it may influence the iron speciation”⁸². In her work she detected considerable amounts of citric, ascorbic, oxalic and succinic acid in potatoes, and that the iron in potatoes was predicted to be mostly soluble and reduced to ferrous. She concluded that the high amount of organic acids present in potatoes is likely to contribute greatly to the bioavailability of the iron present.

Another MSc student who worked on this topic was Melanie Nester. Her work had the topic “Iron distribution in potatoes and assessment of soluted ferrous iron after *in vitro* gastric digestion by use of a newly adapted assay system.”⁸³ Melanie Nester utilized the *in vitro* digestion assay and used it on instant potato powder samples. She has found that during gastric digestion virtually all of the iron is in ferrous form.

2.2) Aim of the project

The aim of this project is to study iron speciation of plant-based foods during the digestion. Different foods will be used, starting with potato. Potato has been chosen because, even though it does not have a particular high amount of iron, it is consumed in large amounts in the UK, being responsible for about 8% of daily iron intake⁸⁴. Potatoes are also rich in organic acids which have been shown to enhance the iron uptake in the gut⁸⁵. Other foods such as peas which have high ferritin content will also be used.

To simulate digestion *in vitro* essays can be used, representing biological conditions, and allowing analysis of iron during the process. Many techniques can be used to analyse the iron in the digested food. Total iron content can be measured with ICP-OES, after being microwave digested. ICP-OES can also be used to

measure the precipitated, nanoparticulated and soluble iron fractions with specific sample preparation, using centrifugation and ultrafiltration.

Ferric and ferrous speciation can be studied with cyclic voltammetry, even though information of the application of this technique to complex matrixes such as food is scarce. Proper methodology will need to be developed, eyeing also ferritin detection and quantification. To develop a working method, simple solutions of ferrous sulphate, ferric chloride and ferritin will be used. Since plant ferritin is not commercially available, it will be isolated from peas in the Plant Sciences Department of the University of Cambridge.

3) Materials and Methods

3.1) Techniques

3.1.1) Microwave digestion

Microwave digestion is a powerful technique in sample preparation. Organic samples, such as food, typically have large sized particles that will damage high sensitivity instruments such as the ICP-OES. With the aid of microwave digestion samples can be homogenised to workable conditions.

The digestion of samples containing organic compounds consists of the establishment of reaction conditions to promote oxidative processes. Three parameters are critical to promote these reactions: the applied temperature, the digestion duration and the acid mixture used for digestion. To achieve the high temperatures required, and to prevent the samples from boiling, high pressure is applied to the reaction chamber.

The common procedure is to use an adequate concentration of nitric acid, sometimes mixed with hydrogen peroxide. Typically the nitric acid is concentrated, as much as 7 mol.L^{-1} , as this yields very good results, normally measured in the residual carbon contents of organic samples. However, based on modern principles of green chemistry, procedures that use strong reaction conditions are being avoided and procedures that achieve the same results while using less reagents, energy and generate less residues are being sought⁸⁶.



Figure 8: Ultrawave microwave digestion equipment, available at MRC-HNR.

3.1.2) ICP-OES

Inductively coupled plasma optical emission spectrometry (ICP-OES) is a popular and powerful analytical tool for the determination of trace elements in extremely varied sample types. Samples need to be in liquid or gaseous states. Solid samples need acid digestion or extraction in order to be present in a solution that can be used. The sample solution is converted into an aerosol and directed into the central channel of the plasma. The plasma has a temperature of approximately 10000 K, quickly vaporising the aerosol and releasing analyte elements as free atoms in gaseous state. Further collisional excitation within the plasma promotes them to excited states. Then, when the ions and atoms return to the ground state energy they release photons, which have characteristic energies. This way we can use the wavelength of the photons to identify the corresponding element, and the number of photons is proportional to the concentration of the element⁸⁷.

In order to collect a measurable signal, a portion of the photons emitted is collected with a lens or concave mirror, forming an image on the entrance aperture of a wavelength detector such as a monochromator. Then the signal is converted to an electrical signal by a photodetector, and subsequently amplified and displayed on a computer. Polychromators are also available and allow the simultaneous detection of up to 70 elements.

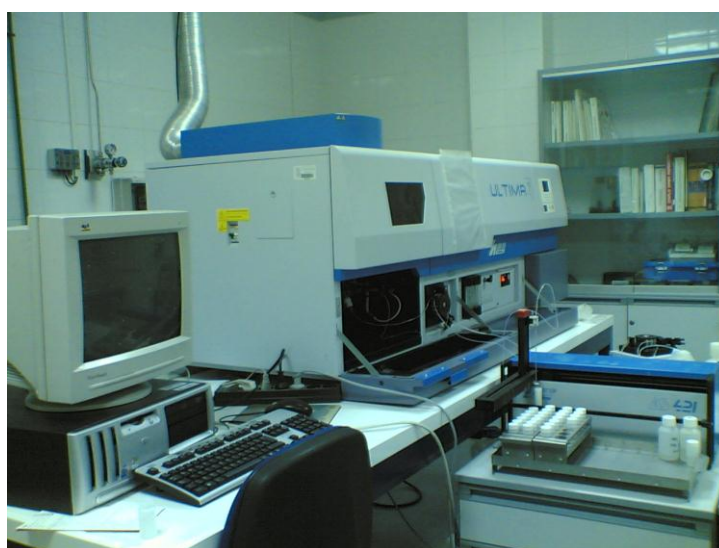


Figure 9: ICP-OES Ultima (Horiba) available at MRC-HNR.

3.2) Materials

3.2.1) Chemicals

Table 5: Chemicals used.

Name	Manufacturer
Amylase	Sigma-Aldrich, UK
Bile bovine	Sigma-Aldrich, UK
Bicinchoninic acid	Sigma-Aldrich, UK
Bradford reagent	Sigma-Aldrich, UK
BSA, albumin from bovine serum	Sigma-Aldrich, UK
Dried peas	Leo, UK
Fresh peas	Tesco, UK
Hydrochloric acid, HCl 37% (w/w)	Sigma-Aldrich, UK
Instant mash potato powder	Smash, Premier Foods, UK
Ferric chloride hexahydrate	Sigma-Aldrich, UK
Ferrous sulphate heptahydrate	Sigma-Aldrich, UK
Magnesium chloride (MgCl ₂)	Fisher Scientific, UK
Nitric acid: ultra-pure HNO ₃ 69 % (w/w)	Sigma-Aldrich, UK
Pancreatin, from porcine pancreas	Sigma-Aldrich, UK
Pepsin, from porcine gastric mucosa	Sigma-Aldrich, UK
Polyvinylpyrrolidone	Fisher Scientific, UK
Potassium dihydrogen phosphate	Sigma-Aldrich, UK
RNase A	Fisher Scientific, UK
Single element solution for ICP, iron solution 1000 ppm in nitric acid	Fisher Scientific, UK
Sodium chloride	Sigma-Aldrich, UK
Sodium hydrogen carbonate	Sigma-Aldrich, UK
Sodium hydroxide	Sigma-Aldrich, UK
Sulphuric acid	Sigma-Aldrich, UK
Trisodium citrate	Sigma-Aldrich, UK

3.2.2) Equipment

Table 6: Equipment used.

Equipment	Name
96 microwell plate	Corning Costar
Balances	Sartorius
Blender	Blender
Centrifuge	Mistral 600, CR 1 C
Electrophoresis	XCell SureLock Mini-Cell
Freeze Drier	LTE Mini Lyotrap
ICP - OES	JY 2000
ICP - OES	JY Ultima
ICP MS/MS	Elan DRS Plus
Microplate reader	Labsystems Multiscan RC
Microwave digestion	Ethos Plus
Potentiostat	Autolab PGSTAT 302N
Rotatory incubator	MB-1000 Incubator
Voltammetry stand	757 Computrace VA Stand

3.3) Methods

Unless otherwise mentioned, all experimental work was performed in the Medical Research Council - Human Nutrition Research in Cambridge, United Kingdom.

3.3.1) Sample preparation

For the potato digestion experiments, the instant potato powder (Figure 10 - A) was used directly without any changes. In the case of the pea digestion experiments, fresh peas (Figure 10 - B) bought from a supermarket were cooked for 3 min in a microwave. Afterwards they were blended with a kitchen blender, and the mash was passed through a sieve with the help of a mortar. The slurry was freeze-dried (LTE Mini Lyotrap) overnight in order to obtain a dry powder, which was used in the *in vitro* digestion experiments. This was done in order to obtain a stable, homogeneous, reproducible sample (*i.e.* a dried powder). For the ferritin extraction, dried peas (Figure 10 - C) purchased from a supermarket were used.



Figure 10: Samples used in this project. A (Left) - instant potato powder, B (Centre) - fresh peas, C (Right) - dried peas

3.3.2) Ferritin extraction

This experiment was performed in the Plant Science Department of the University of Cambridge, with the help of Dr. Janneke Balk. When the procedure demanded, it was carried out in a cold room (4°C). The procedure is adapted from Laulhere et al.⁸⁸.

The phosphate buffer (50 mmolL⁻¹, pH 7.0) was prepared by mixing 30.75 mL of 1 molL⁻¹ K₂HPO₄ and 19.25 mL of 1 molL⁻¹ KH₂PO₄ in ultra-high purity water was added up to 1 litre. The solution was stored at 4°C. Prior to starting the experiment, 10 g of insoluble PVP (polyvinylpolypyrrolidon) was added.

The dried peas (purchased from a supermarket) were ground for 12 s in a coffee grinder. 680 mL of 50 mmolL⁻¹ M phosphate buffer at pH 7.0 with 1% PVP were added. The slurry was ground with a Polytron grinder (10 s, three times), while keeping the sample on ice-water. The slurry was centrifuged for 10 min at 10000 rpm, 2°C. MgCl₂ was added to the supernatant in order to obtain a 50 mmolL⁻¹ concentration, and the solution was then centrifuged (5 min, 5000 rpm, 2°C). The addition of MgCl₂ delayed the precipitation of ferritin as compared with starch and to the bulk of MgCl₂ precipitable proteins⁸⁸. Trisodium acetate was added to make a concentration of 70 mmolL⁻¹ citrate. With this addition of citrate, most of the contaminating proteins were no longer precipitable. RNase A was added and the solution incubated for 2 h at 4°C, with stirring, to help degrade proteins that were not wanted. The solution was centrifuged for 40 min at 13000 rpm. The pellet (rusty-brown) contains the ferritin. Most of the supernatant was removed, and the pellet was resuspended in a small volume of the supernatant, and centrifuged (2 min, 14000 rpm). The supernatant was discarded, and 5 volumes of ultra-high purity water added to the pellet, after which it was centrifuged (2 min, 14000 rpm). The ferritin is in the supernatant (brown colour).

The concentration of this pure ferritin fraction was determined from the total protein content using the Bradford assay combined with iron content analysis by ICP-OES.

3.3.3) Protein content determination

Bradford Protein Assay

This experiment was performed in the Plant Science Department of the University of Cambridge. To perform the Bradford protein assay, the Biorad instructions were followed. A range of protein standards (0, 2.5, 5, 7.5, 10, 15 µg/mL) were prepared with 1 µg/µL bovine serum albumin (BSA) stock solution and ultra-

high purity water. The experimental samples were diluted (1:100 for potato and 1:1000 for pea fractions) in ultra-high purity water. Standards and samples (100 μL each) were mixed with Bio-Rad Protein Assay Dye reagent (900 μL each) previously diluted four times in ultra-high purity water. The absorbance of the solution obtained for the standard and the experimental samples were measured at a wavelength of 595 nm after calibration with ultra-high purity water. The total protein concentration was calculated using the linear regression of the standard curve.

Bicinchoninic Acid Protein Assay

The assay was performed following the manufacturer's (Pierce) protocol. A range of standards (2000, 1500, 1000, 750, 500, 250, 125, 25, 0 $\mu\text{L/mL}$) were prepared from a stock of bovine serum albumin (2 mg/mL in 0.9% saline and 0.05% sodium azide) and ultra-high purity water. A volume of working reagent sufficient for the assay was prepared freshly by mixing 50 parts of bicinchoninic acid (BCA) Reagent A (sodium carbonate, sodium bicarbonate, BCA and sodium tartrate in 0.1 molL^{-1} sodium hydroxide) with 1 part of BCA Reagent B (25 mL with 4% cupric sulphate). All standards and samples (25 μL) were added into a 96 microwell plate in triplicates. Working Reagent (200 μL) was added to each well and the plate was shaken for 30 s using a plate shaker at medium power. The plate was covered and incubated for 30 min at 37°C. The plate was allowed to cool down to room temperature and the absorbance was then measured via a microplate reader (Labsystems Multiskan RC, USA) at wavelength 540 nm. The total protein concentration was calculated using the linear regression of the standard curve.

3.3.4) Determination of iron content (ICP-OES)

In order to measure the concentration of iron in different samples, inductively coupled plasma-optical emission spectrometry (ICP-OES) was used. Prior to analysis all solubilised samples were diluted in 7% HNO_3 (w/w) (pre-prepared from concentrated ultra-pure HNO_3 (69%, w/w) and ultra-high purity water). All dilutions were made by weight using a balance with ± 0.001 g sensitivity. For each set of samples a range of standards appropriate for the expected iron concentration (e.g. 0, 5, 10, 20, 30, 50 ppb) were prepared in 7% HNO_3 from a commercial stock ICP standard (Single Element Solution for ICP iron solution 1000 ppm in 1 molL^{-1} HNO_3).

The standards and samples were nebulised with argon through a concentric nebuliser and introduced through a cyclonic spray chamber into a hot argon plasma torch (up to 7000 K) where the iron was ionised. The photons emitted by the element were detected at the element-specific wavelength (259.94 nm for iron). Every sample and standard was analysed in triplicates. All analyses were run according to alternating measurements of standards-samples-standards. For every raw data set the calibration curve and the standard deviation were verified. All data with >10% relative standard deviation (RSD) were discarded and the analysis repeated.

3.3.5) Microwave-assisted acid digestion

Prior to ICP-OES analysis, solid samples or samples containing precipitates were digested using microwave assisted acid digestion. This was done because only completely solubilized samples can be analysed by ICP-OES.

For this purpose all samples were weighed in the microwave-digestion vessels (0.5 g of sample) and a known amount of ultra-high purity water (2 mL) was added. Then, a volume of 2.5 mL of ultra-pure 69% HNO₃ (w/w) was added. The vessels were sealed and placed in a container with 125 mL of ultra-high purity water and 5 mL of H₂O₂, which was introduced in the microwave. The digestion was performed at 180°C for 15 min following a pre-heating stage. The vessels were allowed to cool to 25°C before the digested samples could be removed. The digested samples were weighed again and then diluted with ultra-high purity water to obtain a final HNO₃ concentration of 7% (w/w). Prior to each microwave digestion run, a clean run was made with only concentrated HNO₃ in the vessels.

3.3.6) *In vitro* digestion assays

Procedure followed

A 1 % of pepsin stock solution (3300 U/mg) was made with 0.2% NaCl. This solution was aliquoted and frozen at -20°C. The pancreatin/bile salt stock solution was prepared fresh for each experiment. Pancreatin (0.24 mg/mL, bile salt (1.5 mg/mL) were added to a 0.1 M NaHCO₃ solution. An amylase solution of 13 U/mg was prepared with 0.2% NaCl. The procedure was adapted from Cilla et al.⁷⁸ and from a previously in-house assay from MRC-HNR (unpublished data), but was

significantly altered. The *in vitro* digestion assays consisted of three phases (Figure 11), representing the different stages of digestion: Buccal digestion, gastric digestion and intestinal digestion. The buccal phase was introduced for the purpose of this specific project.

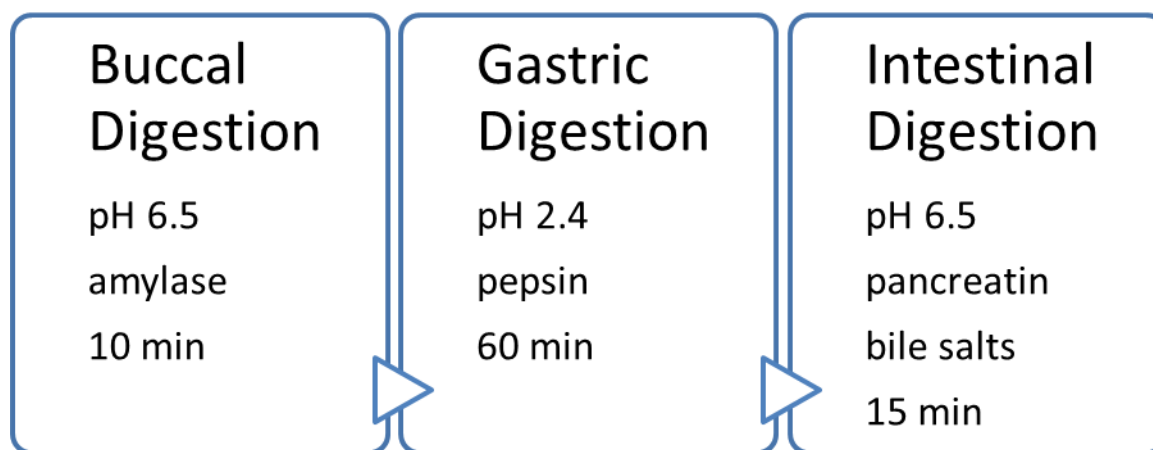


Figure 11: Overview of the *in vitro* digestion system

Buccal phase:

For potato (instant potato powder) and pea (dry powder made from cooked fresh peas) samples, 2 g of sample were used. When spiking (adding a known amount of iron from different sources) was necessary, an amount of ferritin or FeCl_3 which had equivalent iron content to the pea or potato sample was added. 13 ml of 0.2% NaCl and 2 mL of the previously prepared amylase solution were added. The pH was adjusted to 6.5 with 1.5 molL^{-1} HCl and 1 molL^{-1} NaHCO_3 . The mixture was incubated for 10 min in a rotary incubator (MB-1000 Hybridizer) at 37°C , and the pH checked before the next phase.

Gastric Digestion:

15 ml of 0.2% NaCl were added, and the pH adjusted to 2.4 with 1.5 molL^{-1} HCl. 1 mL of pepsin stock solution was added, sufficient to yield 0.02 mg of pepsin/g of sample. The mixture was incubated for 1 h at 37°C in the rotatory incubator. After 1 h aliquots were taken and put on ice for 10 min to stop the enzymatic reactions. Before progressing to the next stage the pH was measured.

Intestinal Phase:

The pH of the digested solution after the gastric phase was increased to 6.5 with the addition of 1 molL⁻¹ NaHCO₃. Freshly prepared pancreatin/bile salt solution sufficient to provide 0.25 mg of pancreatin/mL and 1.5 mg of bile salts/mL was added. This amount was chosen because it was what was found to be optimal by previous work done in the same laboratory⁸³. The mixture was incubated for 15 min in a rotatory incubator at 37°C. Aliquots were then taken and put on ice for 10 min to stop the enzymatic reactions.

Alongside each digestion procedure, a blank solution containing everything except sample was run as a negative control. A FeCl₃ solution was also run each time as a positive control. Each experiment was made with triplicate tubes and repeated 3 times (for a total of 9 samples).

3.3.7) *In vitro* digestion method development and optimization

As mentioned before, the *in vitro* digestion procedure was adapted from Cilla et al.⁷⁸ and from a previously in-house assay from MRC-HNR (unpublished data), but was significantly altered.

The objectives of this method development and optimization were the following:

- 1) Adapt the method to the samples that required analysis (instant potato powder and powder made from cooked fresh peas);
- 2) Obtain a representative consistency in the digested food, that is, obtain a good ratio of sample to buffer had to be achieved. This is essentially a balance between not diluting the sample too much (which would cause problems in quantification by ICP-OES, given the very low levels of iron), and having enough buffer to cover the samples and allow enzyme-sample interactions to occur;
- 3) Introduce a buccal phase. This was deemed important given the starchy nature of potatoes and other vegetables, and the potential effect of amylase;

- 4) Represent the naturally dilution effect that occurs in *in vivo* digestion;
- 5) Optimize the durations of each phase in order to better represent *in vivo* conditions.

In order to work with instant mash potato powder and the powder made from cooked fresh peas, different dilutions of gastric buffer (0.2% NaCl at pH 2.4 with 1.5 molL⁻¹ HCl) were tested, and it was found that the best consistency for the *in vitro* digestion was 0.07 g of instant potato powder per ml of gastric buffer. This allowed efficient mixing and pH measurements without diluting the iron content excessively.

To introduce a buccal phase, different ratios of sample / buffer were experimented and different amounts of amylase. It was concluded that the following worked best:

To start with, 2 g of commercially available instant mash potato powder were added to 13 mL of 0.2% NaCl. Afterwards, 2 mL of the previously prepared amylase solution, at pH 6.5 were added and incubated at 37°C for 10 min in a rotatory incubator (MB-1000 Hybridizer). Then, during gastric digestion more buffer was added, and the pH monitored and adjusted if necessary. In this was the naturally occurring dilution effect was accomplished, and the previously obtained ratio of sample / buffer was respected.

Before optimization the method included one hour of intestinal digestion. Given that iron is absorbed in the duodenum, this allotted time appeared excessive, and was reduced to 15 min.

3.3.8) Iron phase distribution and calculations

For the determination of soluble, precipitated and nanoparticulated iron (Figure 12), the aliquots from different stages of the *in vitro* digestion were first centrifuged at 15000 rpm for 5 min, allowing the collection of the supernatant, which was ultra-filtrated with 3 kDa membrane filters. In cases where further characterization of nanoparticulated content was desired, different sized filters were used (300 kDa and 100 nm filters).

The soluble, nanoparticulate and precipitate phases of iron in suspension were then determined using microwave assisted acid digestion and ICP-OES.

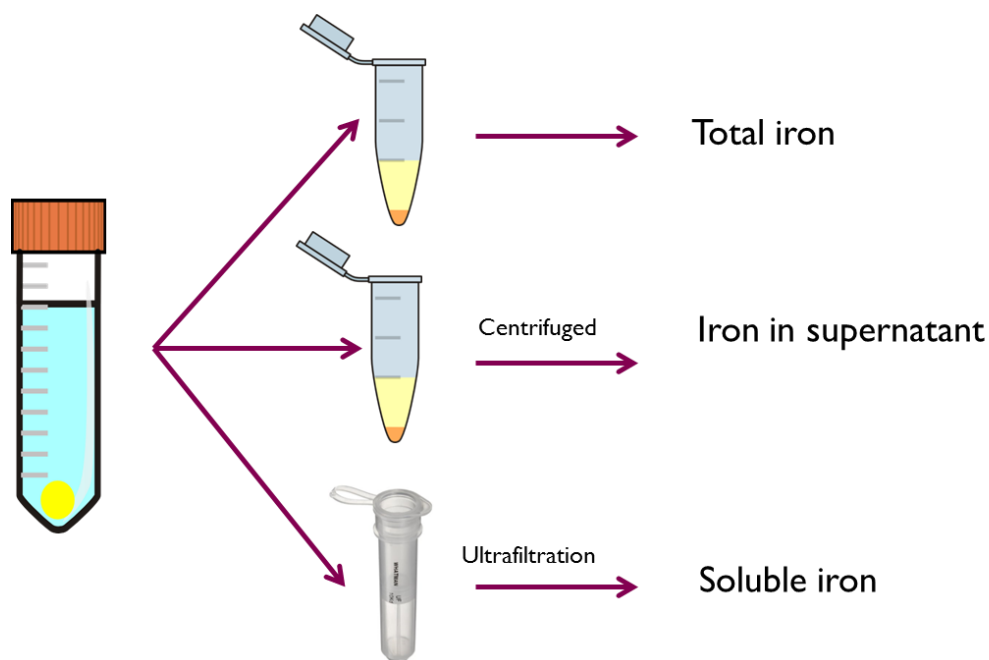


Figure 12: Phase distribution after *in vitro* digestion. After *in vitro* digestion in 50 mL tubes aliquots were taken to 1.5 mL tubes. For total iron quantification, the aliquot was microwave digested before ICP-OES analysis. Other aliquots were centrifuged, and the iron in the supernatant was in some cases quantified and in others ultrafiltered for nanoparticulated iron quantification.

Once the concentration from the ICP-OES is obtained, and verified to have a relative standard deviation inferior to 10%, they are related to the starting amount of iron in the samples. For this to be possible, all steps of the process are quantified by weight, and the dilutions that occur are accounted (see [Figure 13](#) for a typical example).

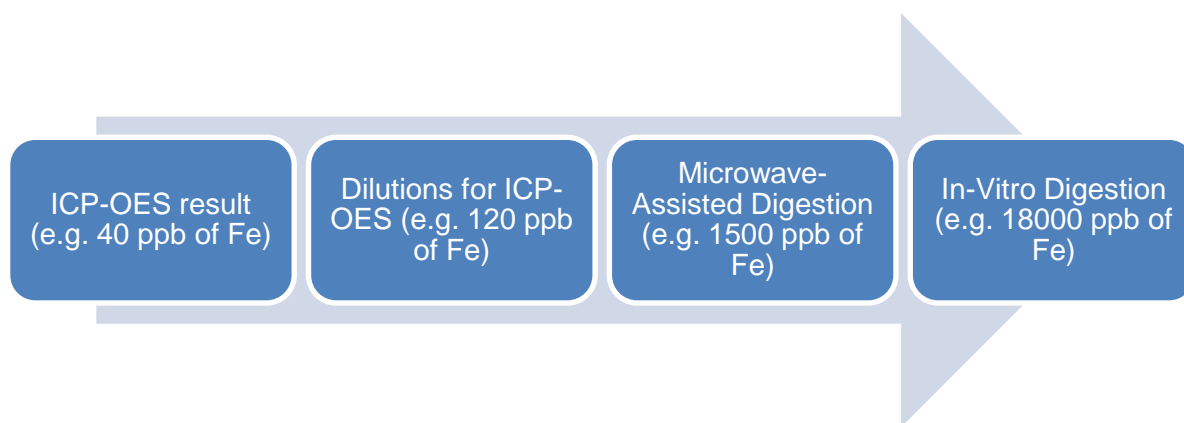


Figure 13: Process behind calculations of Fe content. Typically a result of about 40 ppb of Fe is obtained through ICP-OES analysis. Accounting for all the steps of the process (ICP-OES dilutions in order to obtain a workable level of HNO_3 , microwave assisted digestion and *in vitro* digestion) it is possible to reach the original amount of Fe present in the sample.

After calculating the starting concentrations, the phase distribution relative to the initial sample can be obtained through the following calculations:

$$\% \text{ Soluble} = \text{Soluble Fe} / \text{Total Fe} \times 100$$

$$\% \text{ Precipitated Fe} = (\text{Total Fe} - \text{Supernatant Fe}) / \text{Total Fe} \times 100$$

$$\% \text{ Nanoparticulated Fe} = 100 - (\text{Soluble Fe} / \text{Total Fe} \times 100) - ((\text{Total Fe} - \text{Supernatant Fe}) / \text{Total Fe} \times 100)$$

Regarding the determination of precipitated iron, typically it was calculated by difference from the total iron and the supernatant iron. During methodology development the precipitated iron was calculated directly by centrifugation and microwave digestion of the precipitate. However, since this value always matched the value calculated through subtraction of the supernatant iron from the total iron, it was deemed unnecessary.

3.3.9) SDS-PAGE

Running the gels

Using samples from the *in vitro* digestion of potato powder, (supernatants from the intestinal phase), gel electrophoresis was carried out according to the manufacturer's instructions (Invitrogen). The gel was a NuPAGE Novex Bis-Tris (4-12%) gel, the running buffer was NuPAGE MES, and the sample buffer was NuPAGE LDS Sample Buffer. For each well, 6.5 μ L of sample, 2.5 μ L of sample buffer and 1 μ L of reducing agent (NuPAGE Reducing Agent) were used. In each gel there were 2 negative controls (ultra-high purity water instead of sample) and ferritin positive controls. A protein ladder (BenchMark Pre-Stained Protein Ladder) was also used. Each run was conducted at constant 200 V, and lasted 35 min.

Gel staining

Two different types of staining were used on SDS-PAGE gels. Protein staining was made with a coomassie blue solution (SimplyBlue SafeStain). The gel was washed in ultra-high purity water three times five minutes, and then stained with the staining solution for one hour. Afterwards it was washed overnight with ultra-high purity water.

Iron staining was made by staining overnight with a $K_4[Fe(CN)]_6$ and 2% HCl at room temperature⁸⁹. Different concentration of $K_4[Fe(CN)]_6$ were experimented (2%, 10% and 20%).

3.3.10) Determination of the iron content of the SDS-PAGE Gel Bands

In order to attempt to correlate the protein content present in the bands of the SDS-PAGE gels with iron, the gel was divided and cut into 4 sections of different molecular weight. These sections were microwave digested (see 6.e) with 2 ml of ultra-high purity water and 2.5 mL of 69% HNO_3 (w/w). The digestion lasted 10 min at 180°C, with a ramp up time of 10 min. Following digestion, the samples were diluted with a 30 ppb iridium solution. This iridium solution acts as an internal standard for the ICP-MS/MS instrument. The iron standards prepared had a matching iridium concentration. The iron content was then measured with ICP-MS/MS (Perkin Elmer, Elan DRS Plus).

4. Results and Discussion

4.1) Iron quantification of samples

Before progressing with *in vitro* digestion assays, it was necessary to know exactly how much iron was present in the samples used. To do this, the samples (in powder form) were microwave digested and analysed with ICP-OES.

4.1.1) Potato samples

Different amounts of instant potato powder were microwave digested, diluted and its iron content quantified by ICP-OES. Since in all the different steps the weights were recorded it was possible to calculate the amount of iron present in the starting powder. The iron content was found to be 17.4 ppm ($s=1.5$, $n=8$). The iron content of different batches was tested and found to be consistent. However, it is likely that the amount of iron in this instant potato powder will vary. The amount found is consistent with what previous researchers in the MRC-HNR have found (unpublished data). This value is higher than reported in the literature for fresh potatoes (8.4 ppm)⁵⁷, but this is to be expected since the powder will be more concentrated than real potatoes.

4.1.2) Pea samples

The fresh pea powder that was prepared was also quantified for total Fe content by ICP-OES following microwave digestion. The iron content of the cooked fresh peas powder was found to be 25.3 ppm ($s=0.9$, $n=6$). This result is higher than reported (15.1 ppm)⁵⁷. However, the process of making the fresh peas into a powder will concentrate the iron, and variation in iron content according to origin, maturation and other factors is to be expected.

4.2) Ferritin characterization

After the extraction of ferritin from dried peas performed at the Plant Science Department from the University of Cambridge, about 1.3 mL of resuspended ferritin was obtained. To characterize this extract, that is, to know how loaded each ferritin molecule was with iron, and how much iron in total was present, it was required to do

protein content analysis through a Bradford assay and to quantify the total iron present with ICP-OES. The Bradford assay was performed at the Plant Science Department immediately after the extraction and the iron content analysis in the MRC-HNR at a later date.

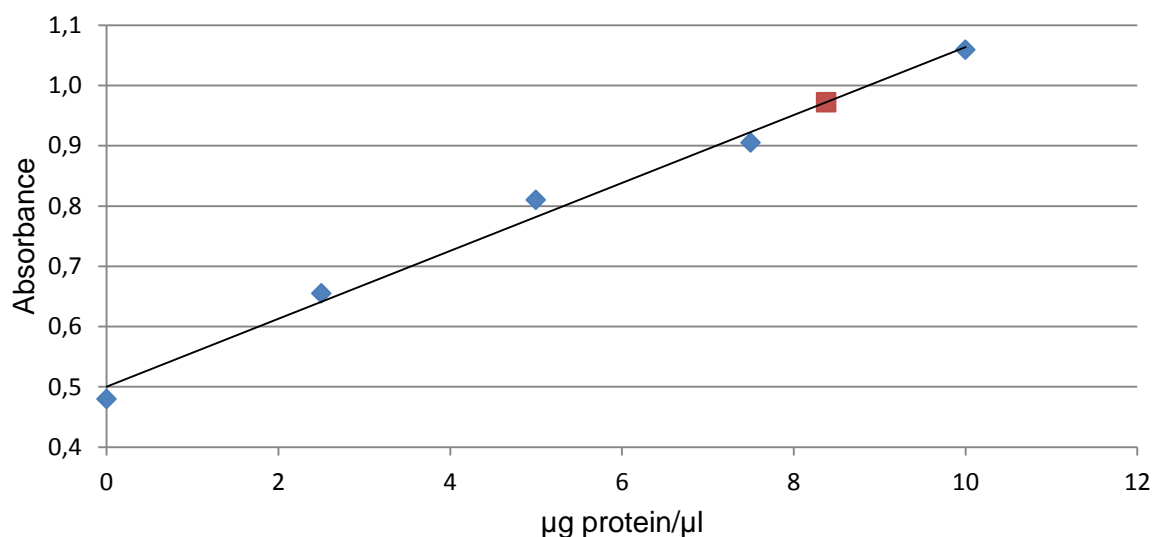


Figure 14: Bradford assay of extracted ferritin. The standards are in blue, and the sample in red.

Through this Bradford assay (Figure 14), it was found that the extracted ferritin had a protein content of 8.38 µg per µl. Given this value, it is estimated that the 1.3 ml of resuspended extracted ferritin have 10.89 mg of protein.

Following protein quantification, iron content quantification was necessary. To accomplish this, a portion of the extracted ferritin was microwave digested and analysed with ICP-OES. It was found that the extracted ferritin had a concentration of iron of 696.0 ppm ($s=0.6$, $n=4$).

With both these results, and knowing that each ferritin usually has 24 subunits of 28 kDa (for a molecular weight of 272 kDa)⁴⁸ it was calculated that each ferritin molecule had 1056 Fe^{3+} ions. The literature reports up to a possible 4000 Fe^{3+} ions stored in each ferritin⁴⁸. The lower amount found is consistent with results from a previous extraction performed in the Plant Science Department of the University of Cambridge previously. It is also worth noting that ferritins of different plants can present different sized subunits⁴⁸.

4.3) *In vitro* digestion assays

To study the speciation of iron during digestion, an *in vitro* digestion assay was used. This assay allows changing many different factors in order to better attempt to replicate *in vivo* digestion. The results from *in vitro* experiments should not be directly comparable with what occurs *in vivo*, but they should provide an idea of what is happening. Some difficult to replicate *in vivo* factors that may change the results are for example the mechanical digestion that occurs along the digestive system, the constant changes of pH during gastric juice secretion, and the presence of other ligands.

It has been shown that measuring the total iron content after *in vitro* digestion does not provide by itself relevant information regarding its bioavailability⁹⁰. Therefore, better characterization of its oxidation state and phase distribution is where the focus is needed.

4.3.1) Behaviour of ferric chloride in the *in vitro* digestion system

In order to validate the results proper controls needed to be established. As a negative control, the same protocol was followed with no sample being introduced. For a positive control, a ferric solution (FeCl_3) with 100 ppm of iron was used. By following the *in vitro* digestion assay described earlier, two time points were studied: after 1 hour of gastric digestion (at pH 2.4, containing amylase and pepsin); and after 15 minutes of intestinal digestion (at pH 6.5, containing pancreatin and bile salts), the following Fe phase distribution was obtained (see [Figure 15](#) and [Table 7](#)) The most relevant time point is after 15 minutes of intestinal digestion, since this attempts to represent the moment when Fe is being absorbed in the duodenum. Given this, in most gastric phases ultrafilters were not used to distinguish between the nano/soluble Fe ratios in the supernatant. In a typical experiment, both the iron distribution between the supernatant and the precipitate in the gastric phase, and among soluble, nanoparticulated and precipitated in the intestinal phase were characterized. This was also for time consuming and cost reasons.

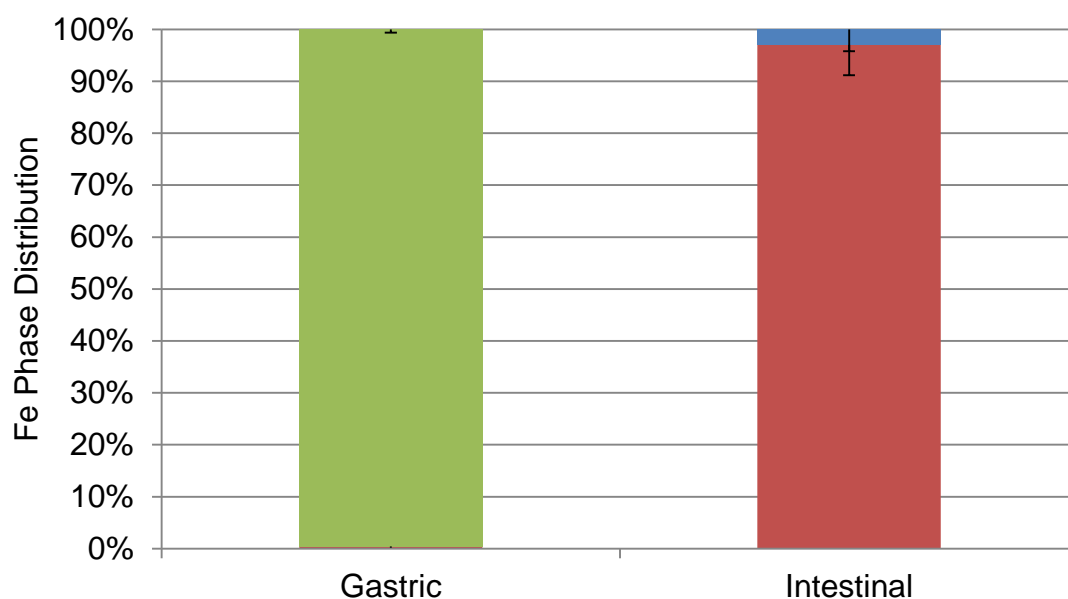


Figure 15: FeCl_3 control Fe phase distribution after *in vitro* digestion, relative to the original amount of Fe expected to be in the sample. Green represents Fe in the supernatant, red the Fe in the precipitate, purple the nanoparticulated Fe and blue the soluble Fe. The gastric phase supernatant Fe was not differentiated between soluble and nanoparticulated with ultrafilters. (Results of three independent experiments, each with $n = 3$)

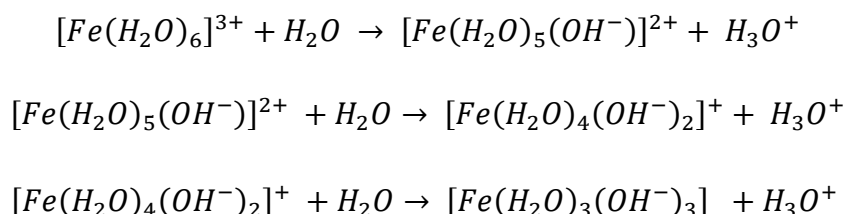
Table 7: FeCl_3 Fe distribution after *in vitro* digestion, relative to what is expected to be in the starting sample.

Fe content (ppm):	Gastric Phase		Intestinal Phase	
	Mean	S.D.	Mean	S.D.
Supernatant	101.56	7.68	-	-
Soluble	-	-	2.88	4.08
Precipitate	0.45	0.63	86.27	15.22
Total	99.46	3.44	89.61	10.50

The reason why total Fe content is not the exact sum of the different phases is because the results presented are averages of different experiments, in which each phase is measured independently.

In gastric conditions all the iron is in the supernatant, given that the low pH of the stomach makes iron soluble in its Fe^{2+} form. In the intestinal phase, the conditions promote the precipitation of iron in ferric form. This precipitation can be

explained by a series of hydrolytic deprotonations that occur to the aquated form of ferric iron (reproduced from section 1.2.2):



4.3.2) Potato digestion

The reason why potatoes were chosen for these studies was because even though they are not a food with a particularly high content of iron, they are widely consumed in the United Kingdom. The reason why the experiments were performed with an instant potato powder and not real potatoes is one of practical nature, since this is a much easier medium to work with.

The instant potato powder contains 17.4 ppm (s=1.5, n= 8) ppm of iron, which is higher than normal fresh potatoes. However, after following the cooking instructions of the instant potato powder, which include a 5 fold dilution, the amount ingested will have about 3.5 ppm of iron. If we account for the natural dilutions that occur during digestion in the stomach⁹¹, the amount of iron present at the duodenum will be circa 1 ppm. Following the *in vitro* digestion assay, the amount of iron present at the intestinal time point will also be about 1 ppm, making it a relevant concentration.

When running instant potato mash samples through the *in vitro* digestion system, the results are quite different, as can be seen in [Figure 16](#) and [Table 8](#).

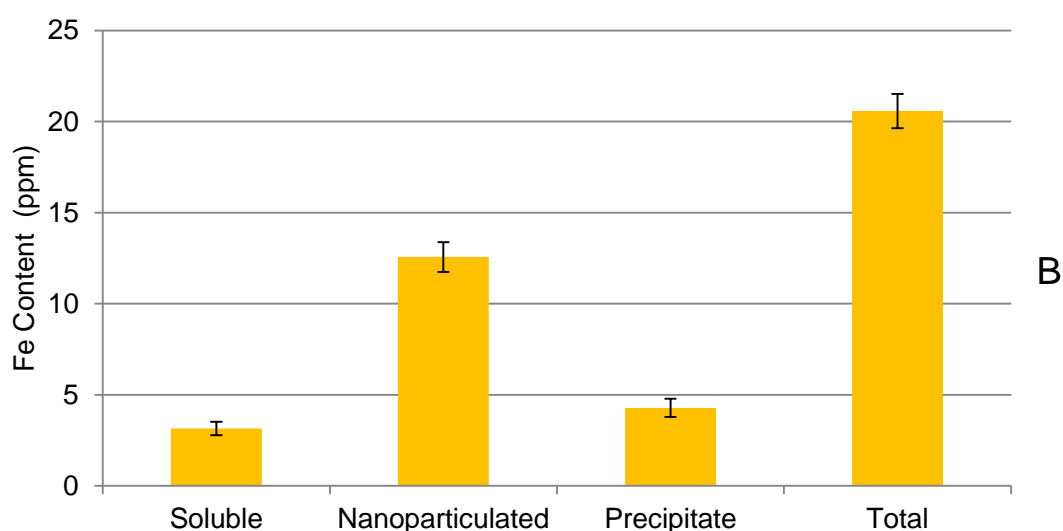
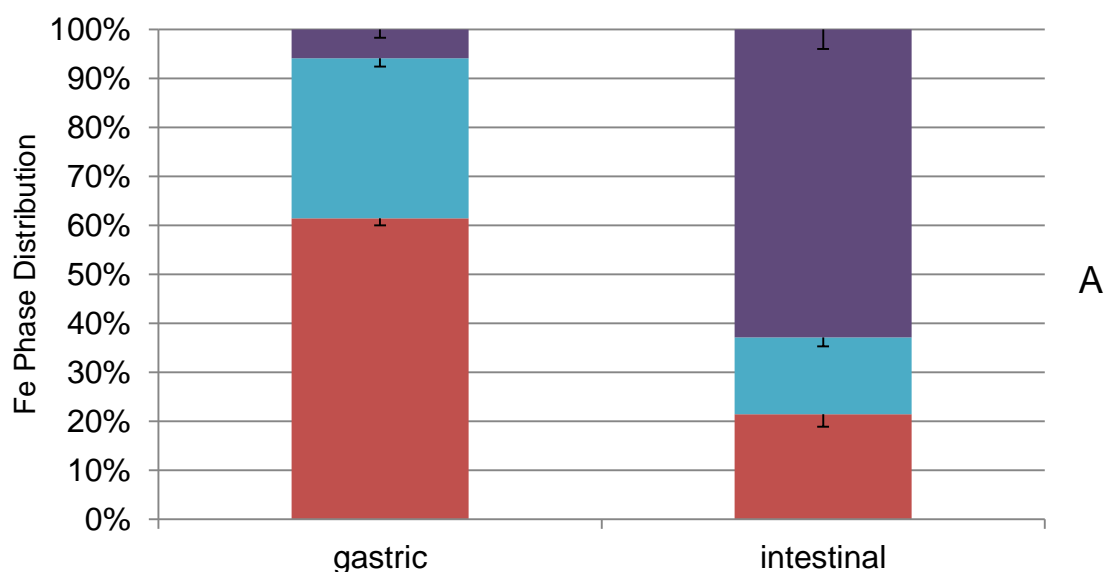


Figure 16: Instant potato powder *in vitro* digestion Fe phase distribution relative to the initial sample (results of three independent experiments, each with n =3). A - (Top) Comparison of the phase distribution in gastric and intestinal conditions. Purple is nanoparticulated Fe, blue represents soluble Fe and red the Fe present in the precipitate. B - (Bottom) Intestinal phase distribution of instant potato powder *in vitro* digestion.

Table 8: Fe distribution after *in vitro* digestion of instant potato powder, relative to the starting sample.

Fe content (ppm):	Gastric Phase		Intestinal Phase	
	Mean	S.D.	Mean	S.D.
Soluble	5.84	0.23	3.14	0.37
Nanoparticulated	1.28	0.23	12.56	0.81
Precipitate	10.14	0.19	4.28	0.50
Total	18.10	0.28	20.58	0.94

The first thing to notice is that what is referred to as “precipitate” is not just precipitated iron, it is the iron that is present, either precipitated or somehow trapped in the yellow pellet (see [Figure 17](#)). Different time points of aliquot collection in the intestinal phase were used, and no significant difference between 15 min and 60 min was found.

The amount of precipitated versus supernatant iron changes in what might be an unexpected fashion between the gastric and intestinal phases. At gastric pH it would be expected that iron would be soluble and at intestinal it would precipitate. It is proposed that part of the iron trapped in the precipitate becomes free when the amylase, both added in the buccal phase and also present in pancreatin becomes active in the intestinal phase. The quantity of the yellow precipitate (everything in the potato powder that has not been dissolved in the buffer) noticeably decreases between gastric and intestinal phase, as can be seen in [Figure 17](#). Still, Fe^{3+} would be expected to precipitate at pH 6.5.



Figure 17: Gastric (left) and intestinal (right) aliquots after *in vitro* digestion. As can be seen, the precipitate includes not only iron. What is referred to as precipitate iron is both normal precipitated iron and also whatever iron is caught in this yellow precipitate.

In previous research done here at MRC-HNR by the Bio Mineral Research group, it was suggested that in intestinal conditions ferric iron would stay out of solution by forming impure Fe^{3+} poly-oxo-hydroxides. It would start hydrolysis but further agglomeration would be prevented by mucin binding. The impurity and instability of these ~10-20 nm Fe nanoparticles would allow lysosomal processing and cellular utilization whilst its initial uptake is made through endocytosis ⁴⁴.

The presence of so much apparent nanoparticulated iron in the intestinal phase of the digestion of the samples is of particular interest, since it agrees with what was proposed by researchers at the MRC-HNR. However, further characterization of what exactly is this “nanoparticulated” iron is needed.

4.3.3) Ferritin digestion

When the ferritin extracted previously is put through the *in vitro* digestion system, all the Fe appears in the supernatant during gastric digestion (see Figure 18 and Table 9). The total values of iron present are high when compared to other experiments because this experiment was done before proper quantification of the iron present in the extracted ferritin was done. In intestinal conditions it presents itself as mostly soluble. One hypothesis for this is that in this *in vitro* system all Fe is released from ferritin during gastric digestion, due to the acidic pH and the enzymes present. However, the results indicate that this Fe does not precipitate in intestinal conditions like the Fe from ferric chloride. Perhaps the amino acids released from the shell of ferritin have an effect preventing the oxidation of the released Fe content and the resultant precipitation.

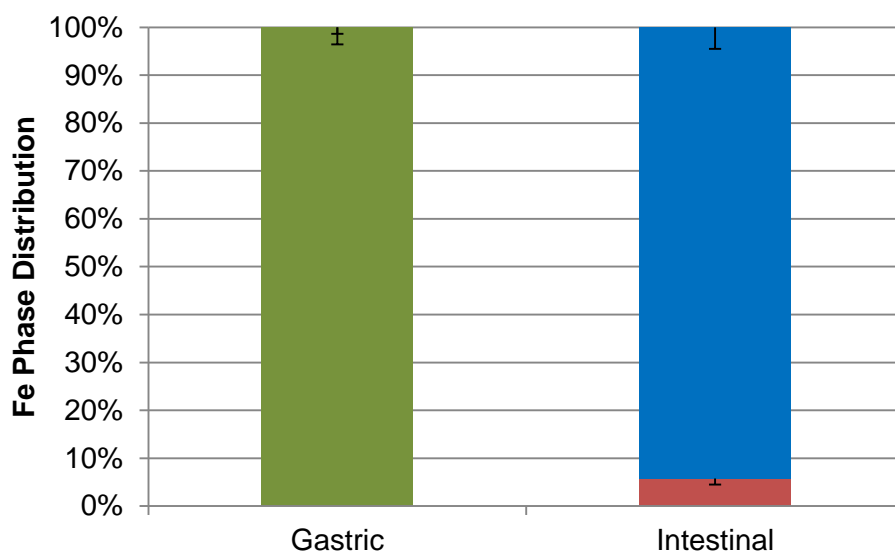


Figure 18: Ferritin *in vitro* digestion Fe phase distribution relative to the initial sample (results of one experiment, with $n = 3$). Green represents the Fe in the supernatant, blue represents soluble Fe and red the Fe present in the precipitate.

Table 9: Fe distribution after *in vitro* digestion of ferritin, relative to the expected starting sample.

Fe content (ppm):	Gastric Phase		Intestinal Phase	
	Mean	S.D.	Mean	S.D.
Supernatant	519.40	18.47		
Soluble			506.02	24.20
Nanoparticulated			0	
Precipitate	0	0	31.04	6.87
Total	480.97	8.48	530.63	12.46

4.3.4) Spiked potato digestion

In previous work done at the MRC-HNR, Melanie Nester has determined considerable amounts of ferritin in potatoes (unpublished data). Ferritin is an iron storage form in plants, and as such it is possible that ferritin may be the main form of iron present in potatoes.

To attempt to understand what happens to ferritin during digestion, an equivalent amount of Fe in the form of ferritin (which was previously extracted from peas) was spiked into the potato powder. The results are as follows in Figure 19 and Table 10:

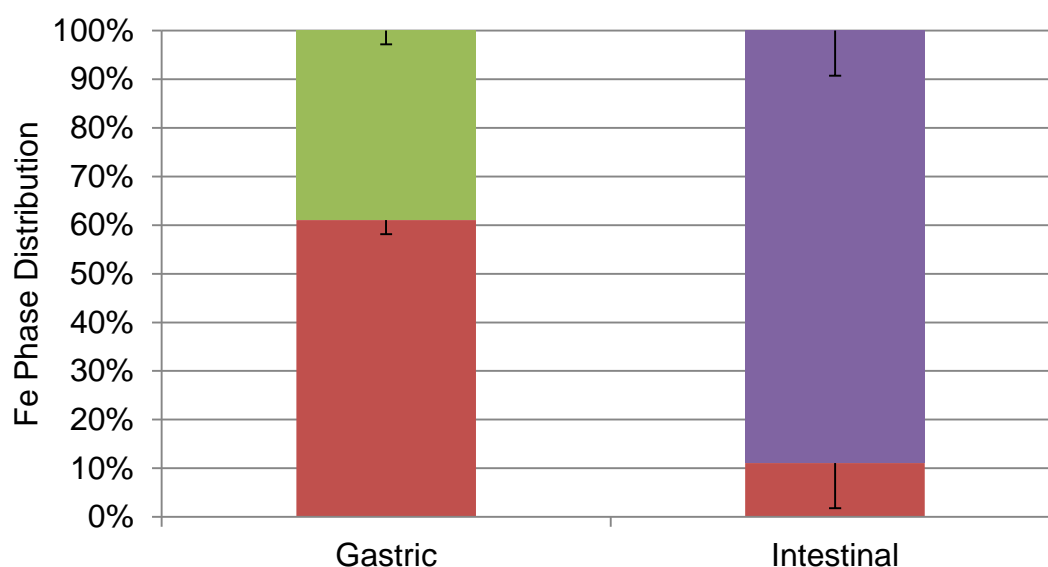


Figure 19: Phase distribution of potato powder spiked with ferritin, relative to the initial sample, (Results of three independent experiments, each with n = 3). Green is the Fe in the supernatant, blue represents soluble Fe, purple is the nanoparticulated Fe and red is the Fe present in the precipitate.

Table 10: Fe distribution after *in vitro* digestion of instant potato powder spiked with ferritin, relative to the starting sample.

Fe content (ppm):	Gastric Phase		Intestinal Phase	
	Mean	S.D.	Mean	S.D.
Supernatant	8.51	0.60	-	-
Soluble	-	-	0	0
Nanoparticulated	-	-	22.64	1.97
Precipitate	17.33	1.94	3.10	3.31
Total	25.50	1.81	26.97	2.53

It is noticeable that when comparing the gastric phases Fe distribution between the digestion of potato and potato spiked with ferritin, the precipitated Fe phase stayed at the same percentage of total Fe, but it increased in absolute terms when the potato was spiked with ferritin. If the Fe in ferritin was not released, it would be expected to manifest itself in the supernatant (nanoparticulated). If it were to be released, it should also be either soluble (possible oxidation of the released ferric iron to ferrous) or nanoparticulated. The presence of part of the iron from ferritin in the precipitated phase could indicate that part of the ferritin was simply trapped in the larger yellow precipitate (Figure 17). It would be interesting to use ultrafiltration in order to characterize the gastric phase when ferritin was spiked as this could have provided more insight to what is happening to ferritin in the gastric phase. In the intestinal phase, the precipitated Fe from the ferritin spike experiment remains virtually the same when compared to the non-spiked experiment. This seems to indicate that all the iron added as ferritin is nanoparticulated in the intestinal phase. This could possibly be from two reasons: either the ferritin did not release its iron content, or it was released in the gastric phase and the ferric iron did not fully precipitate (perhaps due to ligands and organic acids known to be present in potatoes) but stayed in solution in nanoparticulated form.

Another experiment made was to spike the same amount of potato powder with an equivalent amount of Fe in the form of FeCl_3 (Figure 20 and Table 11). This would allow us to see if ferric iron from FeCl_3 would behave in the same way as the iron from ferritin. The results indicate that the added iron behaves in a different manner: it is in the supernatant in the gastric phase (presumably in soluble form) and precipitates in the intestine. The iron from FeCl_3 would be completely soluble in

gastric conditions and immediately precipitate out of solution when exposed to the conditions of the duodenum.

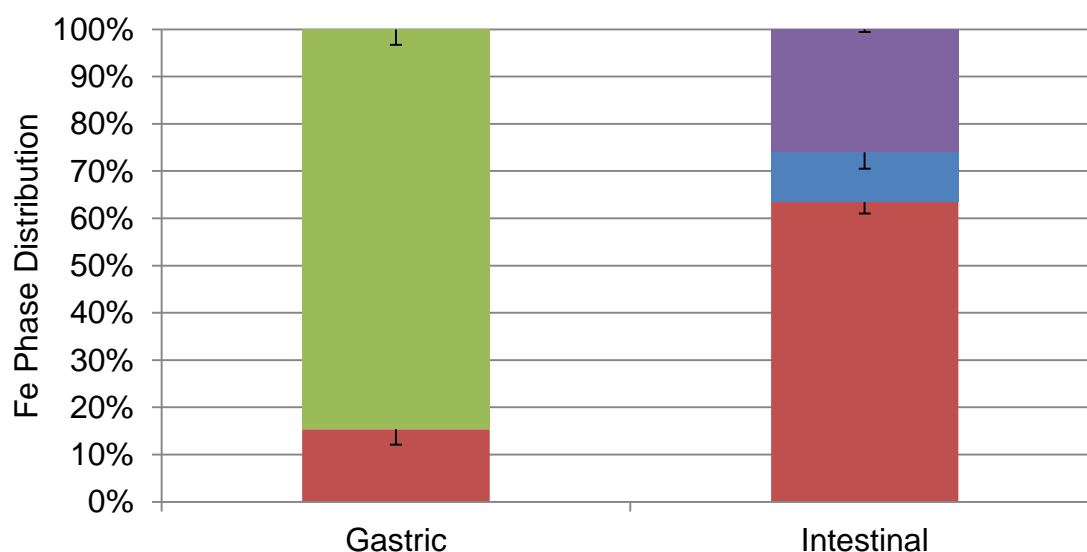


Figure 20: Phase distribution of potato powder spiked with FeCl_3 , relative to the initial sample, (Results of three independent experiments, each with $n = 3$). Green is the Fe in the supernatant, blue represents soluble Fe, purple is the nanoparticulated Fe and red is the Fe present in the precipitate

Table 11: Fe distribution after *in vitro* digestion of instant potato powder spiked with FeCl_3 , relative to the starting sample.

Fe content (ppm):	Gastric Phase		Intestinal Phase	
	Mean	S.D.	Mean	S.D.
Supernatant	34.43	0.65	-	-
Soluble	-	-	4.48	1.05
Nanoparticulated	-	-	11.25	0.06
Precipitate	6.29	1.49	26.95	1.87
Total	40.72	1.14	42.68	1.09

By comparing the *in vitro* digestion of just instant potato powder with instant potato powder spiked with ferritin (Figure 21), we can see that even though the soluble and “precipitated” iron remains relatively the same, the nanoparticulated fraction increases greatly. It appears that virtually all the iron from ferritin is nanoparticulated when in intestinal conditions. By contrast, a spike of FeCl_3 seems to indicate that the spiked iron all precipitates in intestinal conditions.

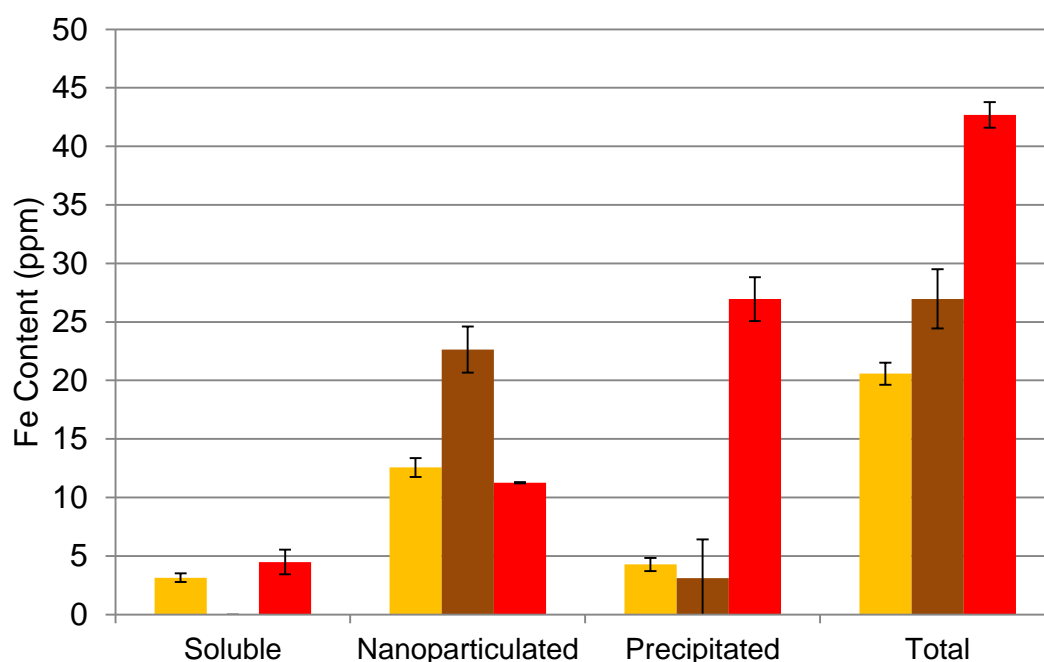


Figure 21: Comparison of different *in vitro* digestion experiments with instant potato powder, at the intestinal time point. Yellow represents just the digestion of instant potato powder, brown represents the potato spiked with ferritin, and red the potato spiked with FeCl₃.

4.3.5) Pea digestion

The same experiments were also carried out with a new, more representative sample: peas. This time, normal fresh peas were used. Peas are known to naturally have a high ferritin content⁸⁸. They were cooked, freeze dried and made into a powder. The results (Figure 22 and Table 12) pointed in the same direction as those in potatoes: In intestinal conditions, most of the iron appears to be nanoparticulated. In both ferritin spike experiments (potatoes and peas) no soluble iron was detected in the intestinal phase.

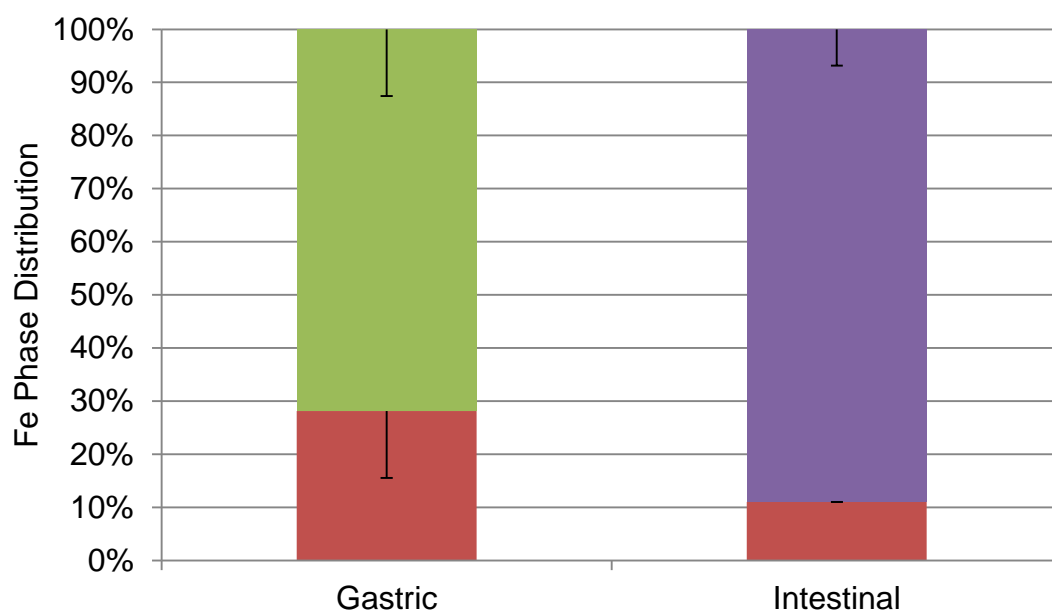


Figure 22: Phase distribution of peas, relative to the initial sample (results of two independent experiments, each with n=3). Green is the Fe in the supernatant, blue represents soluble Fe, purple is the nanoparticulated Fe and red is the Fe present in the precipitate

Table 12: Fe distribution after *in vitro* digestion of peas, relative to the starting sample, (results of two independent experiments, each with n =3).

Fe content (ppm):	Gastric Phase		Intestinal Phase	
	Mean	S.D.	Mean	S.D.
Supernatant	19.28	0.33	-	-
Soluble	-	-	0	0
Nanoparticulated	-	-	22.12	9.32
Precipitate	6.53	2.60	3.30	3.16
Total	25.62	2.28	26.15	1.25

A comparison of the results from the experiments with potato powder and peas can be seen in [Figure 23](#).

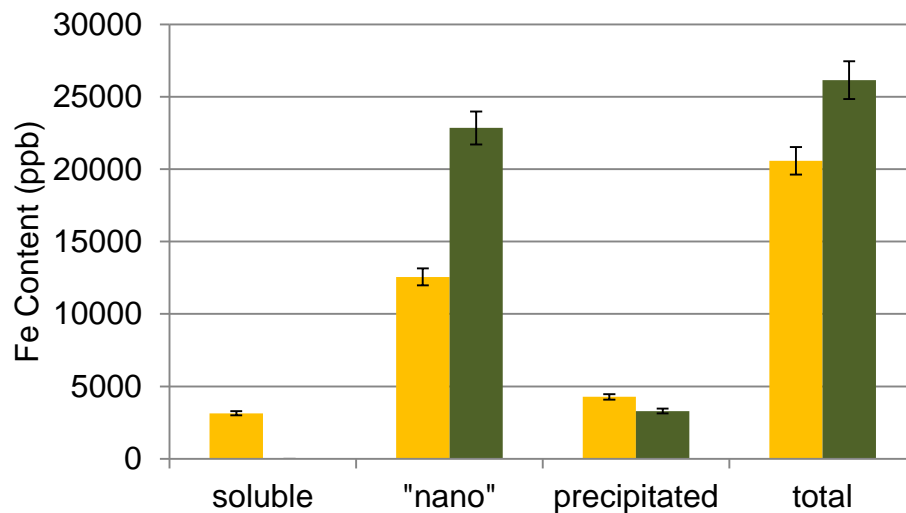


Figure 23: Comparison of the phase distribution of intestinal *in vitro* digested potatoes and peas. The potato experiments are represented in yellow and the peas experiments in green.

4.3.6) Spiked peas digestion

Peas are known to contain a higher content of ferritin when compared with potatoes. This is responsible for their higher content of iron. When spiking peas with ferritin (Figure 24, Figure 25 and Table 13), the same pattern as in potato powder could be observed, that is, the iron from ferritin is present in nanoparticulated form during the absorption time point in the intestine.

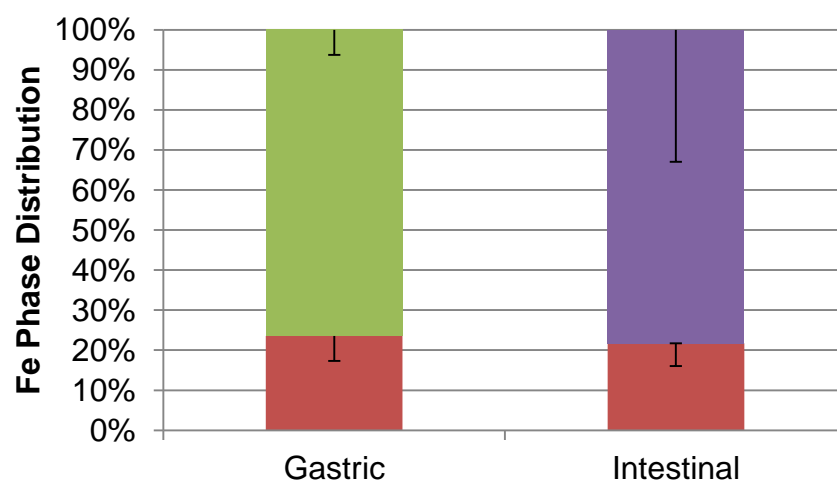


Figure 24: Phase distribution of peas spiked with ferritin, relative to the initial sample (results of two independent experiments, each with $n=3$). Green is the Fe in the supernatant, blue represents soluble Fe, purple is the nanoparticulated Fe and red is the Fe present in the precipitate

Table 13: Fe distribution after *in vitro* digestion of peas spiked with ferritin, relative to the starting sample, (results of two independent experiments, each with n =3)

Fe content (ppm):	Gastric Phase		Intestinal Phase	
	Mean	S.D.	Mean	S.D.
Supernatant	24.37	8.17	-	-
Soluble	-	-	0	0
Nanoparticulated	-	-	26.71	13.10
Precipitate	7.08	0.18	7.78	6.05
Total	32.88	7.99	33.35	1.91

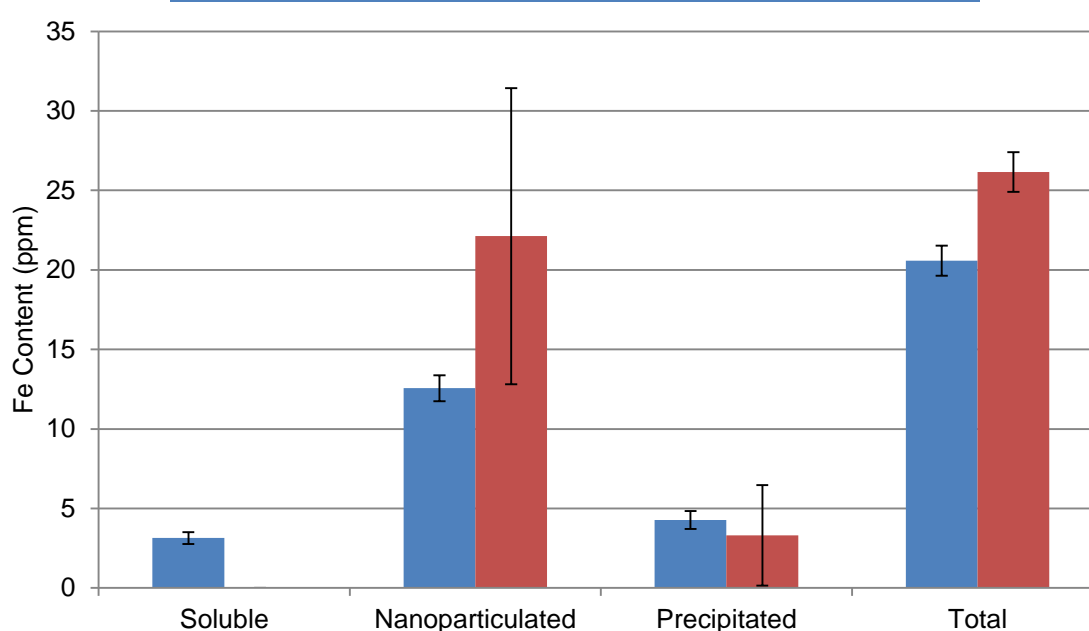


Figure 25: Comparison of the phase distribution of intestinal *in vitro* digested peas and peas spiked with ferritin. The peas experiments are represented in green and the peas spiked with ferritin experiments in red.

4.4) Characterization of the nanoparticulated fraction

4.4.1) Size distribution with ultrafiltration

In order to attempt to characterize the nanoparticulated fraction identified in the intestinal phase (is it iron bound to proteins? Is it iron oxides in the form of nanoparticles? Is it some other form of nanoparticles?), different sized filters were

used to perform ultracentrifugation. The results presented in Figure 26 indicate that the majority of the iron appears to be between the sizes of 3 and 300 kDa. For spherical nanoparticles this would correspond to sizes of about between 2 and 20 nm.

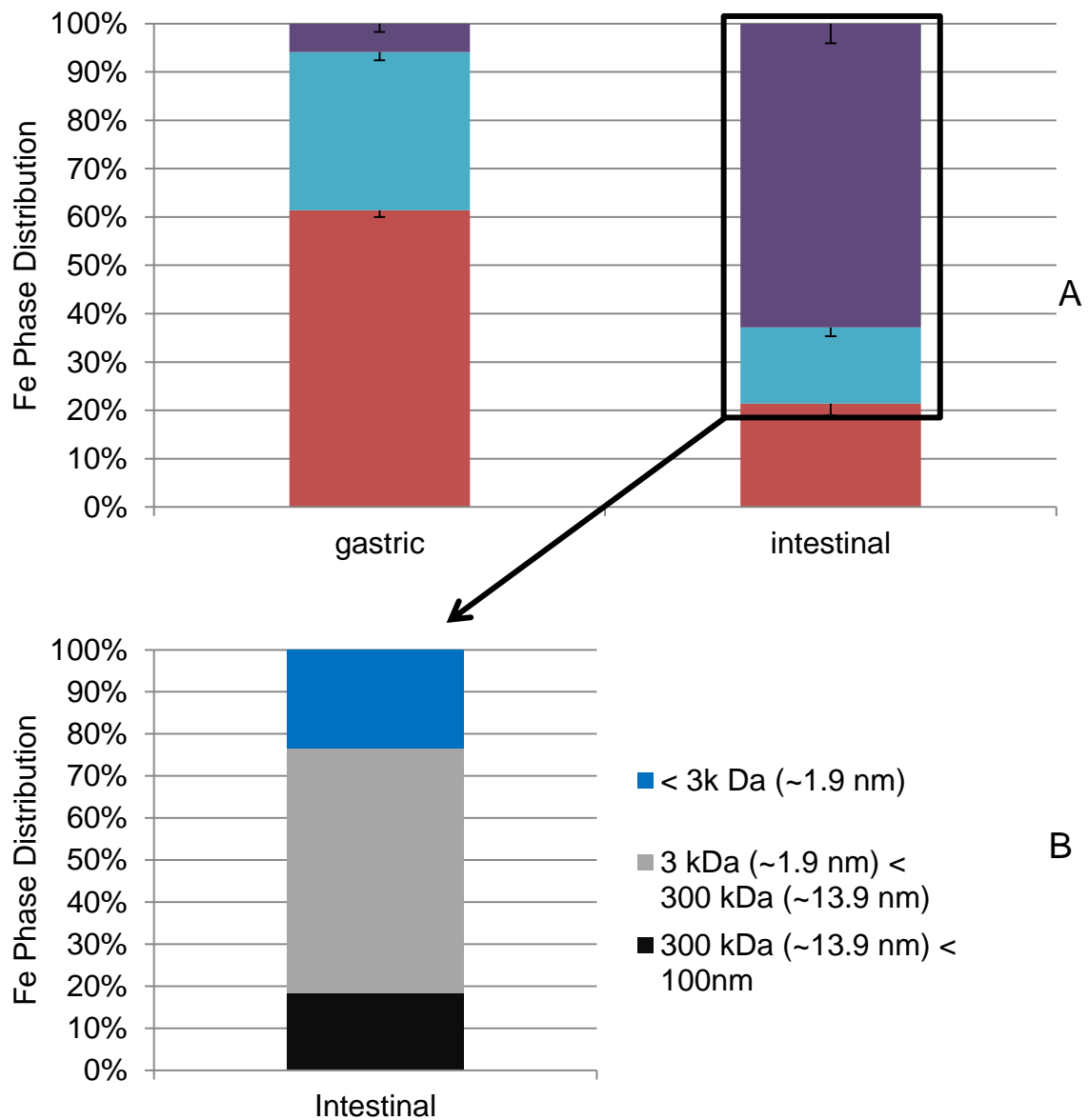


Figure 26: Different sized filters used in the supernatant of the intestinal phase. A- (Top) Phase distribution in gastric and intestinal *in vitro* digestion of potato. Purple is nanoparticulated Fe, blue represents soluble Fe and red the Fe present in the precipitate B- (Bottom) Fe phase distribution of the supernatant of *in vitro* digestion of potato. Blue is soluble Fe (<3 kDa), grey is nanoparticulated Fe (between 3 and 300 kDa) and black is nanoparticulated Fe (between 300 kDa and 100 nm),

Table 14: Fe size distribution of the supernatant of the intestinal phase of an *in vitro* digested potatoes experiment using different sized filters.

Fe content (ppm)	Filter used	Filter size (nm)
9.12	<3 kDa	<2
22.64	3 kDa < 300 kDa	2<14
7.15	300 kDa<100 nm	36<100

4.4.2) Gel electrophoresis

One approach to the characterization of the nanoparticulated Fe fraction identified in the instestinal digestion of the instant potato powder was the following:

- Run a SDS-PAGE and stain it for protein with coomassie blue,
- Cut the gel into 4 different sections with different molecular weights,
- Microwave digest the sections in concentrated acid,
- Quantify the iron present in each section with ICP-MS.

This way it should be possible to correlate the proteins present with the amount of iron at the different molecular weights. The first step to do gel electrophoresis is to quantify the protein content. This will allow the loading of proper quantities in each well of the gel. To do so a BCA protein content test was performed. The standards were made with BSA, and after factoring dilutions a concentration of 7751 µg of protein was obtained (Figure 27).

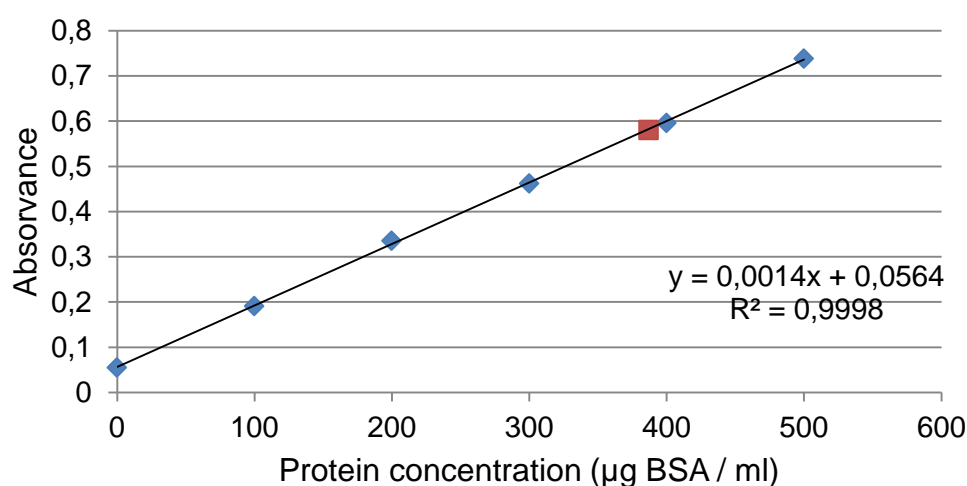


Figure 27: BCA protein content analysis of the supernatant of an intestinal aliquote of a potato *in vitro* digestion. Blue represents the BSA standards and red the sample.

The following were ran in the gels:

- The supernatant of an intestinal aliquot of potato *in vitro* digestion (henceforth called sample in this section);
- Ultra-high purity water as a negative control;
- Ferritin previously isolated from peas;
- The supernatant of an intestinal aliquot of potato *in vitro* digestion spiked with ferritin (an equivalent amount in Fe) prior to the *in vitro* digestion;
- The supernatant of an intestinal aliquot of potato *in vitro* digestion spiked with ferritin (an equivalent amount in Fe) after the *in vitro* digestion.

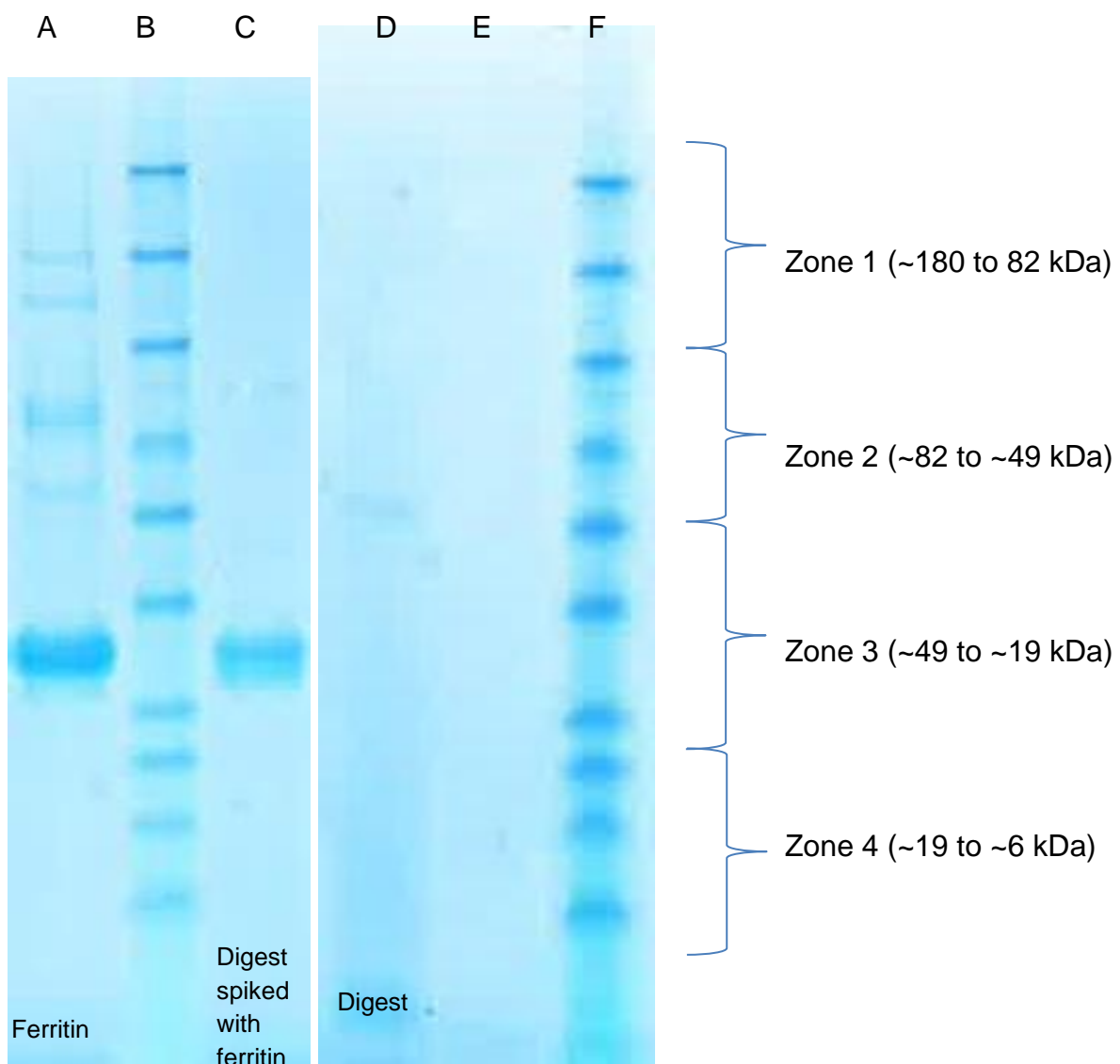


Figure 28: SDS-PAGE stained for protein. Bands B and F are a protein ladder (marker). Band E is a negative control. Band D is the supernatant of an intestinal aliquot of a potato *in vitro* digestion. Band A is ferritin, and Band C the supernatant of an intestinal aliquot of potato *in vitro* digestion spiked with ferritin (an equivalent amount in Fe) after the *in vitro* digestion.

In the bands of ferritin, sample, and sample spiked with ferritin after the *in vitro* digestion, two bands were visible, at ~26 kDa and ~48 kDa. 28 kDa is the typical molecular weight of a subunit of plant ferritin⁴⁸. The 10 bands of the marker (protein ladder) have the following molecular weights: 6, 15, 19, 26, 37, 49, 64, 82, 115 and 180 kDa.

After cutting the gel in four different sections ([Figure 28](#)), microwave digesting them and analysing through ICP-MS, the results obtained are in [Figure 29](#).

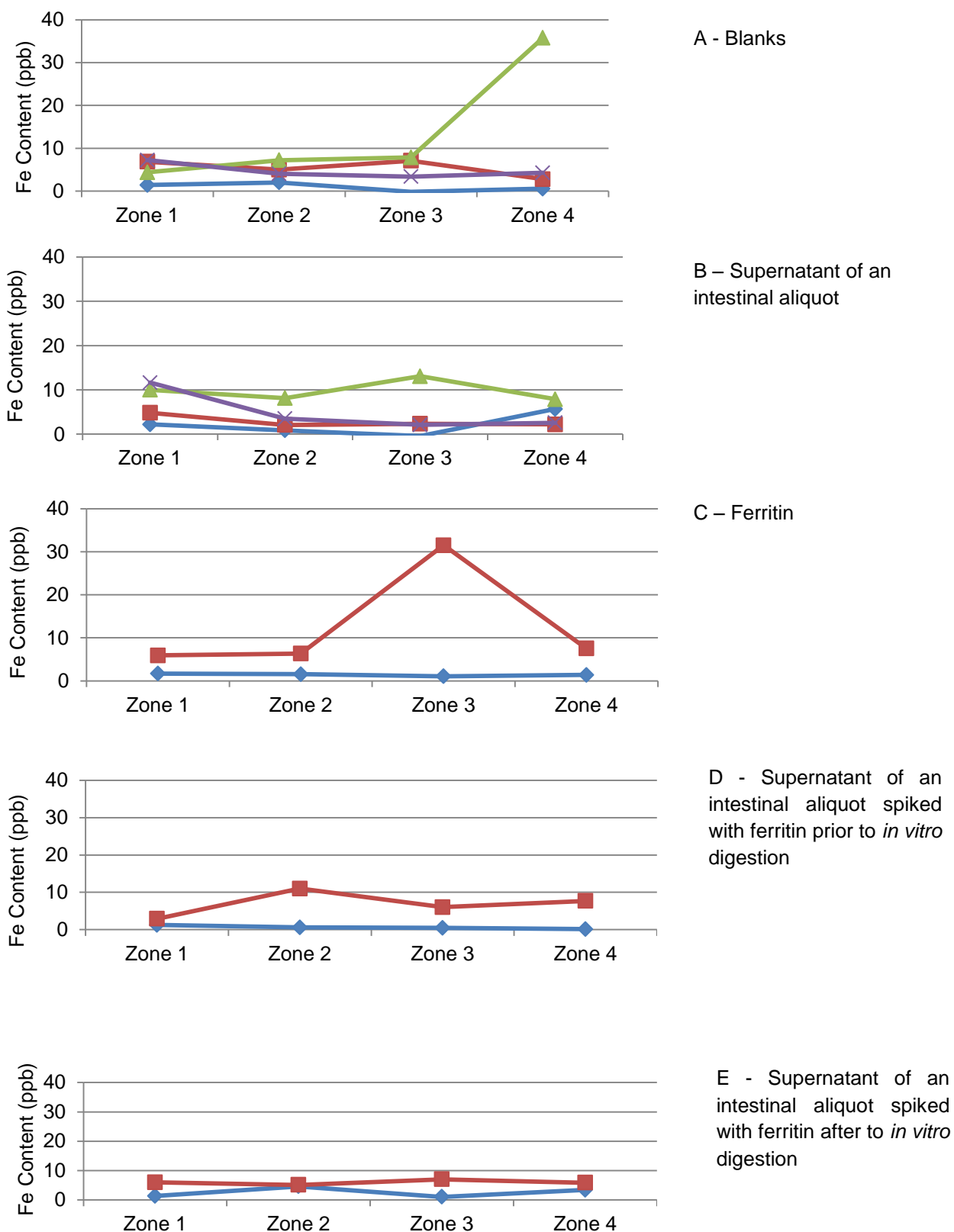


Figure 29: Fe content of SDS-PAGE gels measured by ICP-MS. The gels are cut in four different sections. Different colours are replicates. A - Blanks, B - Supernatant of an intestinal aliquot of potato *in vitro* digestion (sample), C- Ferritin, D- Sample spiked with ferritin prior to *in vitro* digestion, E - Sample spiked with ferritin after *in vitro* digestion.

As can be seen in [Figure 29](#), the results are not very conclusive. There is too much variation even between gels run in parallel, and a proper blank could not be established. Some possible reasons for this are:

- Use of a novel approach that needs to be optimized. Measuring SDS-PAGE gels through ICP-MS had not been done before at the MRC-HNR.
- Extremely low levels. Measurements of a few ppb of Fe were typical, and at this level any contamination can be of great significance. For example, even using the highest purity nitric acid available there is always some Fe contamination present inside.

Conclusions

- 1) An *in vitro* digestion system was adapted and optimized for the study of plant-based foods. The studies made in this system indicate that both potatoes and peas are a good source of bioavailable iron and thus can help in the prevention of iron deficiency.
- 2) Building on work previously developed at the MRC-HNR, the iron phase distribution of instant potato powder and cooked fresh peas was determined, and at the absorption site (duodenum) the *in vitro* studies point to a prevalence of iron in nanoparticulated form. To characterize these nanoparticles, different sized filters were used and pointed to the majority of this iron nanoparticles being between the sizes of 2 and 14 nm. To further characterize this phase, gel electrophoresis with different stains coupled with ICP analysis were attempted but did not provide conclusive results.
- 3) Iron from FeCl_3 and ferritin behaves in different ways when spiked on a plant-based food such as potatoes or peas and digested *in vitro*. Ferric iron from FeCl_3 precipitated when in intestinal conditions, thus being unavailable for absorption while ferritin was present as nanoparticulated iron at the duodenum, either because the ferric iron content was not released during gastric digestion, or it was released and formed other nanoparticles.
- 4) Future work would necessarily focus on characterising conclusively what the nanoparticulated iron found at the intestinal level is. The gel electrophoresis work done in this project can be optimized to deal with the low levels of iron present and might provide a better understanding of the size of the nanoparticles. Techniques such as Single Particle ICP-MS, size exclusion chromatography and laser ablation ICP-MS can help this characterisation.
- 5) Further work on voltammetry, possibly using ligands and progressing to the study of more complex matrixes might be able to study in real time the redox behaviour of iron during an *in vitro* digestion.

- 6) Other interesting future work will be not only the study of different plant-based foods but also the study of full meals, in order to understand how the interaction of different foods alters the speciation and consequently the bioavailability of iron.

References

1. Truswell, J. M. S., *Essentials of Human Nutrition*. 2nd edition ed.; Oxford University Press: 1998.
2. Forbes, A., Iron and Parenteral Nutrition. *Gastroenterology* **2009**, *137* (5), S47-S54.
3. Conrad, M. E.; Umbreit, J. N., Pathways of Iron Absorption. *Blood Cells, Molecules, and Diseases* **2002**, *29* (3), 336-355.
4. Finch, C. A.; Ragan, H. A.; Dyer, I. A.; Cook, J. D., Body iron loss in animals. *Proceedings of the Society of Experimental Biology and Medicine* **1978**, *159* (3), 335-8.
5. Conrad, M. E.; Weintraub, L. R.; Crosby, W. H., The Role of the Intestine in Iron Kinetics. *Journal of Clinical Investigation* **1964**, *43*, 963-74.
6. Crosby, W. H.; Conrad, M. E., Jr.; Wheby, M. S., The Rate of Iron Accumulation in Iron Storage Disease. *Blood* **1963**, *22*, 429-40.
7. Andrews, N. C., Medical progress: Disorders of iron metabolism. *New England Journal of Medicine* **1999**, *341* (26), 1986-1995.
8. Prasad, A. S., *Trace elements and iron in human metabolism*. Plenum Medical Book Co.: 1978.
9. Haemoglobin structure.
http://www.elm.manchester.ac.uk/pub_projects/2001/MNQC7NDS/hb3.jpg (accessed 22/11/2012).
10. Kilmartin, J. V.; Rossi-Bernardi, L., The binding of carbon dioxide by horse haemoglobin. *Biochemistry Journal* **1971**, *124* (1), 31-45.
11. Gorman, D.; Drewry, A.; Huang, Y. L.; Sames, C., The clinical toxicology of carbon monoxide. *Toxicology* **2003**, *187* (1), 25-38.
12. Lu, M.; Wang, H.; Li, X. F.; Lu, X.; Cullen, W. R.; Arnold, L. L.; Cohen, S. M.; Le, X. C., Evidence of hemoglobin binding to arsenic as a basis for the accumulation of arsenic in rat blood. *Chemical Research in Toxicology* **2004**, *17* (12), 1733-42.
13. Ordway, G. A.; Garry, D. J., Myoglobin: an essential hemoprotein in striated muscle. *Journal of Experimental Biology* **2004**, *207* (Pt 20), 3441-6.
14. Balk, J.; Pilon, M., Ancient and essential: the assembly of iron–sulfur clusters in plants. *Trends in Plant Science* **2011**, *16* (4), 218-226.
15. Bych, K.; Kerscher, S.; Netz, D. J.; Pierik, A. J.; Zwicker, K.; Huynen, M. A.; Lill, R.; Brandt, U.; Balk, J., The iron-sulphur protein Ind1 is required for effective complex I assembly. *Embo Journal* **2008**, *27* (12), 1736-46.

16. WHO/UNICEF/ICCIDD, *Iron deficiency anemia: assessment, prevention and control*. World Health Organization: 2001.
17. Fischbacher, C.; Bhopal, R.; Patel, S.; White, M.; Unwin, N.; Alberti, K. G. M. M., Anaemia in Chinese, South Asian, and European populations in Newcastle upon Tyne: cross sectional study. *British Medical Journal* **2001**, 322 (7292), 958-959.
18. Grantham-McGregor, S.; Ani, C., A review of studies on the effect of iron deficiency on cognitive development in children. *Journal of Nutrition* **2001**, 131 (2), 649S-666S.
19. Reddy, S.; Adcock, K. J.; Adeshina, H.; Cooke, A. R.; Akene, J.; Mc, F. H., Immunity, transferrin, and survival in kwashiorkor. *British Medical Journal* **1970**, 4 (5730), 268-70.
20. Seshadri, S.; Gopaldas, T., Impact of iron supplementation on cognitive functions in preschool and school-aged children: the Indian experience. *American Journal of Clinical Nutrition* **1989**, 50 (3 Suppl), 675-84.
21. Soemantri, A. G., Preliminary findings on iron supplementation and learning achievement of rural Indonesian children. *American Journal of Clinical Nutrition* **1989**, 50 (3 Suppl), 698-701.
22. Pollitt, E.; Hathirat, P.; Kotchabhakdi, N. J.; Missell, L.; Valyasevi, A., Iron deficiency and educational achievement in Thailand. *American Journal of Clinical Nutrition* **1989**, 50 (3 Suppl), 687-96.
23. Hershko, C.; Karsai, A.; Eylon, L.; Izak, G., The effect of chronic iron deficiency on some biochemical functions of the human hemopoietic tissue. *Blood* **1970**, 36 (3), 321-9.
24. Basta, S. S.; Soekirman; Karyadi, D.; Scrimshaw, N. S., Iron deficiency anemia and the productivity of adult males in Indonesia. *American Journal of Clinical Nutrition* **1979**, 32 (4), 916-25.
25. Lone, F. W.; Qureshi, R. N.; Emanuel, F., Maternal anaemia and its impact on perinatal outcome. *Tropical Medicine & International Health* **2004**, 9 (4), 486-490.
26. Gardner, G. W.; Edgerton, V. R.; Senewiratne, B.; Barnard, R. J.; Ohira, Y., Physical work capacity and metabolic stress in subjects with iron deficiency anemia. *American Journal of Clinical Nutrition* **1977**, 30 (6), 910-7.
27. Davies, C. T.; Chukweumeka, A. C.; Van Haaren, J. P., Iron-deficiency anaemia: its effect on maximum aerobic power and responses to exercise in African males aged 17-40 years. *Clinical Science* **1973**, 44 (6), 555-62.
28. Judisch, J. M.; Naiman, J. L.; Oski, F. A., The fallacy of the fat iron-deficient child. *Pediatrics* **1966**, 37 (6), 987-90.

29. Aukett, M. A.; Parks, Y. A.; Scott, P. H.; Wharton, B. A., Treatment with iron increases weight gain and psychomotor development. *Archives of Diseases in Childhood* **1986**, 61 (9), 849-57.
30. Beard, J.; Tobin, B.; Green, W., Evidence for thyroid hormone deficiency in iron-deficient anemic rats. *Journal of Nutrition* **1989**, 119 (5), 772-8.
31. Klopffleisch, R.; Olias, P., The Pathology of Comparative Animal Models of Human Haemochromatosis. *Journal of Comparative Pathology* **2012**, 147 (4), 460-478.
32. Lieu, P. T.; Heiskala, M.; Peterson, P. A.; Yang, Y., The roles of iron in health and disease. *Molecular Aspects of Medicine* **2001**, 22 (1–2), 1-87.
33. Roberts, S. K.; Henderson, R. W.; Young, G. P., Modulation of uptake of heme by rat small intestinal mucosa in iron deficiency. *American Journal of Physiology* **1993**, 265 (4 Pt 1), G712-8.
34. Sharp, P.; Srai, S. K., Molecular mechanisms involved in intestinal iron absorption. *World Journal Gastroenterology* **2007**, 13 (35), 4716-24.
35. Hallberg, L.; Brune, M.; Rossander, L., Iron absorption in man: ascorbic acid and dose-dependent inhibition by phytate. *American Journal of Clinical Nutrition* **1989**, 49 (1), 140-4.
36. Han, O.; Failla, M. L.; Hill, A. D.; Morris, E. R.; Smith, J. C., Jr., Reduction of Fe(III) is required for uptake of nonheme iron by Caco-2 cells. *Journal of Nutrition* **1995**, 125 (5), 1291-9.
37. Glahn, R. P.; Van Campen, D. R., Iron uptake is enhanced in Caco-2 cell monolayers by cysteine and reduced cysteinyl glycine. *Journal of Nutrition* **1997**, 127 (4), 642-7.
38. Swain, J. H.; Tabatabai, L. B.; Reddy, M. B., Histidine content of low-molecular-weight beef proteins influences nonheme iron bioavailability in Caco-2 cells. *Journal of Nutrition* **2002**, 132 (2), 245-51.
39. Raja, K. B.; Simpson, R. J.; Peters, T. J., Investigation of a role for reduction in ferric iron uptake by mouse duodenum. *Biochimica et Biophysica Acta* **1992**, 10 (2), 141-6.
40. McKie, A. T.; Barrow, D.; Latunde-Dada, G. O.; Rolfs, A.; Sager, G.; Mudaly, E.; Mudaly, M.; Richardson, C.; Barlow, D.; Bomford, A.; Peters, T. J.; Raja, K. B.; Shirali, S.; Hediger, M. A.; Farzaneh, F.; Simpson, R. J., An iron-regulated ferric reductase associated with the absorption of dietary iron. *Science* **2001**, 291 (5509), 1755-9.
41. Gunshin, H.; Mackenzie, B.; Berger, U. V.; Gunshin, Y.; Romero, M. F.; Boron, W. F.; Nussberger, S.; Gollan, J. L.; Hediger, M. A., Cloning and characterization of a mammalian proton-coupled metal-ion transporter. *Nature* **1997**, 388 (6641), 482-8.
42. Tandy, S.; Williams, M.; Leggett, A.; Lopez-Jimenez, M.; Dedes, M.; Ramesh, B.; Srai, S. K.; Sharp, P., Nramp2 expression is associated with pH-dependent iron

- uptake across the apical membrane of human intestinal Caco-2 cells. *Journal of Biological Chemistry* **2000**, 275 (2), 1023-9.
43. Su, M. A.; Trenor, C. C.; Fleming, J. C.; Fleming, M. D.; Andrews, N. C., The G185R mutation disrupts function of the iron transporter Nramp2. *Blood* **1998**, 92 (6), 2157-63.
 44. Pereira, D.; Mergler, B.; Faria, N.; Bruggaber, S.; Poots, L.; Latunde-Dada, G.; Simpson, R.; Lönnerdal, B.; Brown, A.; J, P., Gut epithelial cell acquisition of iron(III) invokes a nano-endocytic pathway without iron redox activity. *Unpublished* **2012**.
 45. Theil, E. C. B., Jean-Francois, *Plant ferritin and non-heme iron nutrition in humans*. International Food Policy Research Institute & International Center for Tropical Agriculture 2004.
 46. Davila-Hicks, P.; Theil, E. C.; Lonnerdal, B., Iron in ferritin or in salts (ferrous sulfate) is equally bioavailable in nonanemic women. *American Journall of Clinical Nutrition* **2004**, 80 (4), 936-40.
 47. Murray-Kolb, L. E.; Welch, R.; Theil, E. C.; Beard, J. L., Women with low iron stores absorb iron from soybeans. *American Journall of Clinical Nutrition* **2003**, 77 (1), 180-4.
 48. Harrison, P. M.; Arosio, P., The ferritins: molecular properties, iron storage function and cellular regulation. *Biochimica et Biophysica Acta (BBA) - Bioenergetics* **1996**, 1275 (3), 161-203.
 49. Lonnerdal, B., Soybean ferritin: implications for iron status of vegetarians. *American Journall of Clinical Nutrition* **2009**, 89 (5), 8.
 50. Weintraub, L. R.; Weinstein, M. B.; Huser, H. J.; Rafal, S., Absorption of hemoglobin iron: the role of a heme-splitting substance in the intestinal mucosa. *Journal of Clinical Investigation* **1968**, 47 (3), 531-9.
 51. Parmley, R. T.; Barton, J. C.; Conrad, M. E.; Austin, R. L.; Holland, R. M., Ultrastructural cytochemistry and radioautography of hemoglobin--iron absorption. *Experimental Molecular Pathology* **1981**, 34 (2), 131-44.
 52. Andrews, N. C.; Schmidt, P. J., Iron homeostasis. *Annual Review of Physiology* **2007**, 69, 69-85.
 53. McKie, A. T.; Marciani, P.; Rolfs, A.; Brennan, K.; Wehr, K.; Barrow, D.; Miret, S.; Bomford, A.; Peters, T. J.; Farzaneh, F.; Hediger, M. A.; Hentze, M. W.; Simpson, R. J., A novel duodenal iron-regulated transporter, IREG1, implicated in the basolateral transfer of iron to the circulation. *Molecular Cell* **2000**, 5 (2), 299-309.
 54. Vulpe, C. D.; Kuo, Y. M.; Murphy, T. L.; Cowley, L.; Askwith, C.; Libina, N.; Gitschier, J.; Anderson, G. J., Hephaestin, a ceruloplasmin homologue implicated in intestinal iron transport, is defective in the sla mouse. *Nature Genetics* **1999**, 21 (2), 195-9.

55. Zhang, D.; Lee, H. F.; Pettit, S. C.; Zaro, J. L.; Huang, N.; Shen, W. C., Characterization of transferrin receptor-mediated endocytosis and cellular iron delivery of recombinant human serum transferrin from rice (*Oryza sativa* L.). *Biotechnology* **2012**, 12 (1), 92.
56. Thomas, D., A study on the mineral depletion of the foods available to us as a nation over the period 1940 to 1991. *Nutritional Health* **2003**, 17 (2), 85-115.
57. Bruggaber, S. F.; Chapman, T. P.; Thane, C. W.; Olson, A.; Jugdaohsingh, R.; Powell, J. J., A re-analysis of the iron content of plant-based foods in the United Kingdom. *British Journal of Nutrition* **2012**, 1, 1-8.
58. Kongkachuichai, R.; Napatthalung, P.; Charoensiri, R., Heme and Nonheme Iron Content of Animal Products Commonly Consumed in Thailand. *Journal of Food Composition and Analysis* **2002**, 15 (4), 389-398.
59. Human Vitamin and Mineral Requirements.
<http://www.fao.org/docrep/004/Y2809E/y2809e0j.htm> (accessed 10-12-12).
60. Aisen, P.; Enns, C.; Wessling-Resnick, M., Chemistry and biology of eukaryotic iron metabolism. *International Journal of Biochemistry & Cell Biology* **2001**, 33 (10), 940-959.
61. Dailey, H. A.; Finnegan, M. G.; Johnson, M. K., Human ferrochelatase is an iron-sulfur protein. *Biochemistry* **1994**, 33 (2), 403-407.
62. Taketani, S.; Kakimoto, K.; Ueta, H.; Masaki, R.; Furukawa, T., Involvement of ABC7 in the biosynthesis of heme in erythroid cells: interaction of ABC7 with ferrochelatase. *Blood* **2003**, 101 (8), 3274-80.
63. Bauminger, E. R.; Harrison, P. M.; Hechel, D.; Hodson, N. W.; Nowik, I.; Treffry, A.; Yewdall, S. J., Iron (II) oxidation and early intermediates of iron-core formation in recombinant human H-chain ferritin. *Biochemistry Journal* **1993**, 296 (Pt 3), 709-19.
64. Theil, E. C., Iron homeostasis and nutritional iron deficiency. *Journal of Nutrition* **2011**, 141 (4), 23.
65. Fleming, M. D.; Romano, M. A.; Su, M. A.; Garrick, L. M.; Garrick, M. D.; Andrews, N. C., Nramp2 is mutated in the anemic Belgrade (b) rat: evidence of a role for Nramp2 in endosomal iron transport. *Proceedings of the National Academy of Science of the United States of America* **1998**, 95 (3), 1148-53.
66. Park, C. H.; Bacon, B. R.; Brittenham, G. M.; Tavill, A. S., Pathology of dietary carbonyl iron overload in rats. *Laboratorial Investigation* **1987**, 57 (5), 555-63.
67. Halliwell, B.; Gutteridge, J. M., Role of free radicals and catalytic metal ions in human disease: an overview. *Methods Enzymology* **1990**, 186, 1-85.

68. McCloy, R. F.; Greenberg, G. R.; Baron, J. H., Duodenal pH in health and duodenal ulcer disease: effect of a meal, Coca-Cola, smoking, and cimetidine. *Gut* **1984**, 25 (4), 386-92.
69. Bates, G. W.; Billups, C.; Saltman, P., The kinetics and mechanism of iron (3) exchange between chelates and transferrin. II. The presentation and removal with ethylenediaminetetraacetate. *Journal of Biological Chemistry* **1967**, 242 (12), 2816-21.
70. Beard, J. L.; Burton, J. W.; Theil, E. C., Purified ferritin and soybean meal can be sources of iron for treating iron deficiency in rats. *Journal of Nutrition* **1996**, 126 (1), 154-60.
71. Skikne, B.; Fonzo, D.; Lynch, S. R.; Cook, J. D., Bovine ferritin iron bioavailability in man. *European Journal of Clinical Investigation* **1997**, 27 (3), 228-33.
72. Layrisse, M.; Martinez-Torres, C.; Renzy, M.; Leets, I., Ferritin iron absorption in man. *Blood* **1975**, 45 (5), 689-98.
73. Hoppler, M.; Schonbachler, A.; Meile, L.; Hurrell, R. F.; Walczyk, T., Ferritin-iron is released during boiling and in vitro gastric digestion. *Journal of Nutrition* **2008**, 138 (5), 878-84.
74. Kapsokefalou, M.; Miller, D. D., Iron speciation in intestinal contents of rats fed meals composed of meat and nonmeat sources of protein and fat. *Food Chemistry* **1995**, 52 (1), 47-56.
75. Yvon, M.; Beucher, S.; Scanff, P.; Thirouin, S.; Pelissier, J. P., In vitro simulation of gastric digestion of milk proteins: comparison between in vitro and in vivo data. *Journal of Agricultural and Food Chemistry* **1992**, 40 (2), 239-244.
76. Savoie, L.; Charbonneau, R.; Parent, G., In vitro amino acid digestibility of food proteins as measured by the digestion cell technique. *Plant Foods Human Nutrition* **1989**, 39 (1), 93-107.
77. Englyst, K. N.; Englyst, H. N.; Hudson, G. J.; Cole, T. J.; Cummings, J. H., Rapidly available glucose in foods: an in vitro measurement that reflects the glycemic response. *American Journal of Clinical Nutrition* **1999**, 69 (3), 448-54.
78. Cilla, A.; Perales, S.; Lagarda, M. J.; Barbera, R.; Farre, R., Iron bioavailability in fortified fruit beverages using ferritin synthesis by Caco-2 cells. *Journal of Agricultural and Food Chemistry* **2008**, 56 (18), 8699-703.
79. Granfeldt, Y.; Bjorck, I.; Drews, A.; Tovar, J., An in vitro procedure based on chewing to predict metabolic response to starch in cereal and legume products. *European Journal of Clinical Nutrition* **1992**, 46 (9), 649-60.
80. Urooj, A.; Puttraj, S., Digestibility index and factors affecting rate of starch digestion in vitro in conventional food preparation. *Nahrung* **1999**, 43 (1), 42-7.

81. Hoebler, C.; Lecannu, G.; Belleville, C.; Devaux, M. F.; Popineau, Y.; Barry, J. L., Development of an in vitro system simulating bucco-gastric digestion to assess the physical and chemical changes of food. *International Journal of Food Science Nutrition* **2002**, 53 (5), 389-402.
82. Embacher, K. The organic acid profile of the potato vacuole analyzed by capillary electrophoresis and how it may influence the iron speciation. Technical University of Munich, 2012.
83. Nester, M. Iron distribution in potatoes and assessment of soluted ferrous iron after *in vitro* gastric digestion by use of a newly adapted assay system. Technical University of Munich, 2011.
84. Munoz, M.; Garcia-Erce, J. A.; Remacha, A. F., Disorders of iron metabolism. Part II: iron deficiency and iron overload. *Journal of Clinical Pathology* **2011**, 64 (4), 287-296.
85. Embacher, K. The organic acid profile of the potato vacuole analysed by capillary electrophoresis and how it may influence the iron speciation. Technische Universität München, 2011.
86. Nobrega, J. A.; Pirola, C.; Fialho, L. L.; Rota, G.; de Campos Jordao, C. E.; Pollo, F., Microwave-assisted digestion of organic samples: how simple can it become? *Talanta* **2012**, 98, 272-6.
87. Hou, X.; Jones, B. T., *Inductively Coupled Plasma-Optical Emission Spectrometry*. John Wiley & Sons, Ltd: 2006.
88. Laulhere, J. P.; Laboure, A. M.; Briat, J. F., Mechanism of the transition from plant ferritin to phytosiderin. *Journal of Biological Chemistry* **1989**, 264 (6), 3629-35.
89. Bettedi, L.; Aslam, M. F.; Szular, J.; Mandilaras, K.; Missirlis, F., Iron depletion in the intestines of Malvolio mutant flies does not occur in the absence of a multicopper oxidase. *Journal of Experimental Biology* **2011**, 214 (Pt 6), 971-8.
90. Hallberg, L.; Hulthen, L., Prediction of dietary iron absorption: an algorithm for calculating absorption and bioavailability of dietary iron. *American Journal of Clinical Nutrition* **2000**, 71 (5), 1147-60.
91. Biology, C. C. Digestive System.
<http://biology.clc.uc.edu/courses/bio105/digestiv.htm> (accessed 27/06/2013).